VOL [ 21 ] ISSUE [ 04 ]

# NEWSLETTER

Space Telescope Science Institute

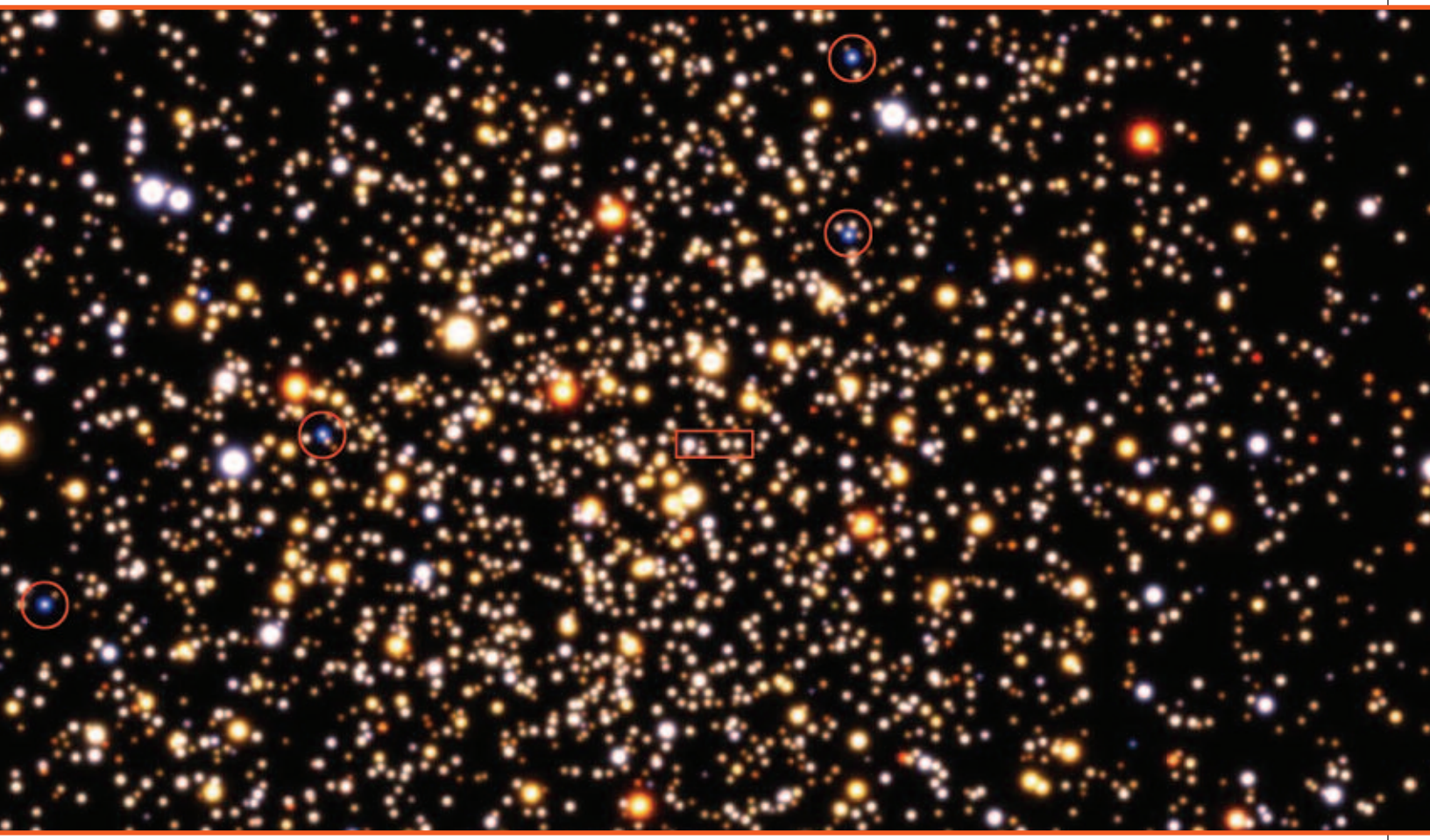

Image of the open cluster NGC 6791, courtesy of E.M. Green. Caption for this figure is located on page 5.

## STIS Situation

**R. Doxsey,** *doxsey@stsci.edu*, **S. Beckwith,** *svwb@stsci.edu*

### Power Supply Failure

On Tuesday, August 3, 2004, an anomaly in the Space Telescope Imaging Spectrograph (STIS) caused the instrument to autonomously enter a "suspend" state, which shut off some components and suspended STIS observations. Initial indications were that a five-volt power supply had failed. The Hubble Project Office at Goddard Space Flight Center (GSFC) led the team analyzing the anomaly, including engineers from GSFC, Ball Aerospace (builders of STIS), and Interpoint (builders of the power supply). An official failure review board continues the analysis and has confirmed the power supply has failed. The board will evaluate possible work-arounds, recommend any testing necessary to verify the failure hypothesis, and look for additional damage that might have occurred during the failure.

All other science instruments—and the observatory itself—continue to function normally.

*Continued page 3*

## Mid-Ultraviolet Spectral Templates for Old Stellar Systems

**R. Peterson,** *peterson@ucolick.org*, **B. Carney, B. Dorman, E. Green, W. Landsman, J. Liebert, R. O'Connell, R. Rood, & R. Schiavon**

The goal of our three-year Treasury Program is to provide observational and theoretical templates for understanding the age, metallicity, and populations of galaxies and stellar clusters as young as 1 Gyr from their mid-ultraviolet (UV) spectra (2200 Å to over 3150 Å). Our products should be applicable to objects as diverse as extragalactic globular clusters in Virgo and high-redshift systems such as Extremely Red Objects seen in the Hubble Ultra-Deep Field (UDF) and other surveys. Here we summarize the status of our contribution, with emphasis on our theoretical calculations and how well they match real data. We can now model the mid-UV and optical spectra of stars of near-solar metallicity well enough that we can refine abundances of trace species in standard stars and constrain age and metallicity in extragalactic globular clusters.

*Continued page 5*

FALL [ 2004 ]

# Going to Plan B?

**S. Beckwith,** *svwb@stsci.edu*

It was a black day for the *Hubble* community on January 16 when Sean O'Keefe, NASA's administrator, announced that we would no longer send humans to *Hubble* to keep it productive; it was too risky. We had been reminded of those risks when the space shuttle *Columbia* burned up a year earlier on a mission to enable humans to carry out experiments in space. Now we realized the significance of *Hubble*'s reliance on risking human life for its scientific success.

Mr. O'Keefe's announcement triggered a public outcry that was unique for a pure science project. Newspaper editorials around the world questioned the wisdom of continuing to fly the space shuttle while refusing to service *Hubble*. Congress weighed in with resolutions in both houses calling for a second opinion. The National Academy of Sciences, at NASA's request, convened a prestigious panel of experts in science, engineering, and spaceflight under the chairmanship of Louis Lanzerotti to consider the case for continued *Hubble* servicing by any means, including the traditional shuttle flights.

At the same time, NASA began to search for alternative ways of keeping its most recognized icon alive. The agency issued a call for ideas to do what we have done since the dawn of civilization: find a way to use machines to carry out the risky work deemed undesirable for humans. On August 13, Mr. O'Keefe announced that NASA will pursue the development of robotic servicing for Servicing Mission 4 (SM4). It looks well within our grasp to replace the astronauts with a robot to carry out the most critical tasks originally planned for SM4. There is a ray of hope for the *Hubble* community, sending machines to fix our machines in space.

To be sure, upgrading the scientific instruments with robots will be technically more challenging than sending astronauts. There are open questions about the wisdom of opening the doors to the instrument bays necessary to replace the Corrective Optics Space Telescope Axial Replacement with the Cosmic Origins Spectrograph. Also, there is concern about several tasks planned for SM4 that might be dropped from a robotic mission, most notably changing one of the Fine Guidance Sensors and installing the Aft Shroud Cooling System. Nevertheless, robotic servicing confers some advantages over humans, the most important being no practical limit to the time needed to carry out some of the complex tasks. Astronauts must do everything within five six-hour spacewalks.

It remains to be seen if the technical developments will come soon enough to rescue *Hubble* before its batteries go dead. The team at Goddard Space Flight Center is convinced they can do it, and the team certainly includes the best possible people to meet this daunting challenge. The history of civilization is punctuated with tools invented to do what we cannot do easily by ourselves; machines repairing machines is the next logical step.

The Lanzerotti committee has yet to issue their final report. An interim letter from the committee to Mr. O'Keefe strongly endorsed the future scientific value of *Hubble* and recommended both human and robotic servicing be maintained as options until a future assessment of the technical readiness of the robotics can be carried out. We at the Institute are committed to support the recommendations of the Lanzerotti committee. If NASA heeds their advice, we may have an even better chance of seeing SM4 carried out than we did before Mr. O'Keefe's announcement in January.

Can NASA lead the next major shift in the technological revolution by developing robots to service its machines in space? I hope so. It presents us with at least two viable options for keeping *Hubble* alive: use of the space shuttle or robotic servicing with technology NASA would like to have in any case for its future missions. A successful robotic servicing mission would be *Hubble*'s second big triumph of ingenuity over adversity, allowing our most powerful eye on the heavens to continue to inspire us for many years to come. Ω

*STIS Situation from page 1*

The failed unit delivers power to all the mechanisms in STIS, including the slit and grating wheels, and the CCD shutter. Because STIS was idle at the time of the failure, the light path was blocked, a precaution to prevent potential exposure of the detectors to excessive light. Without the failed power supply, the STIS mechanisms cannot be moved.

As with the other *Hubble* instruments, STIS has some redundant components. STIS was operating on the "side-1" electronics from launch through May 2001, when a short circuit developed somewhere in the side-1 electronics and blew a fuse. At that time, operations of STIS were switched to use the side-2 electronics. The failure of the five-volt power supply in the side-2 electronics leaves STIS inoperable. (The fuse blown by the side-1 failure was replaced during the last servicing mission, but we believe the short circuit remains.)

## Impact of STIS Failure by Science Category

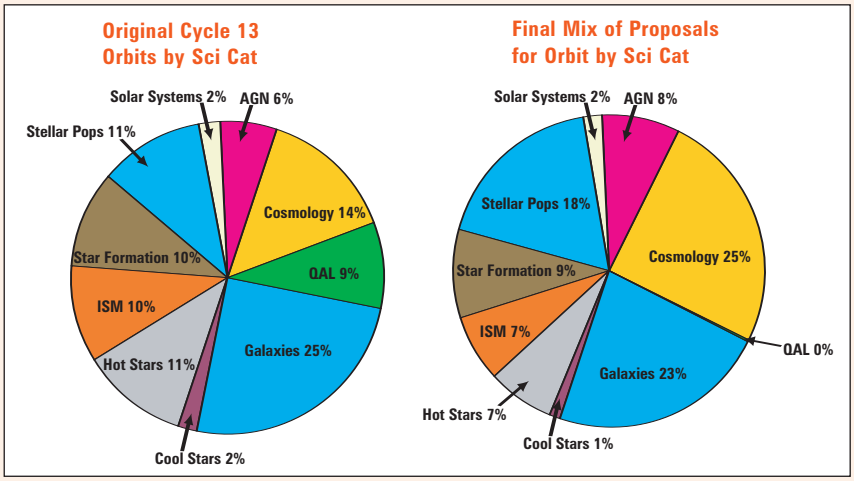


**Figure 1:** Distributions of telescope time by scientific category, as originally awarded in Cycle 13 (left) and after the replacement of STIS programs (right). The primary changes are a reduction in studies of quasar absorption lines and a growth in studies of stellar populations and cosmology.

## Institutional Acceptance Rate

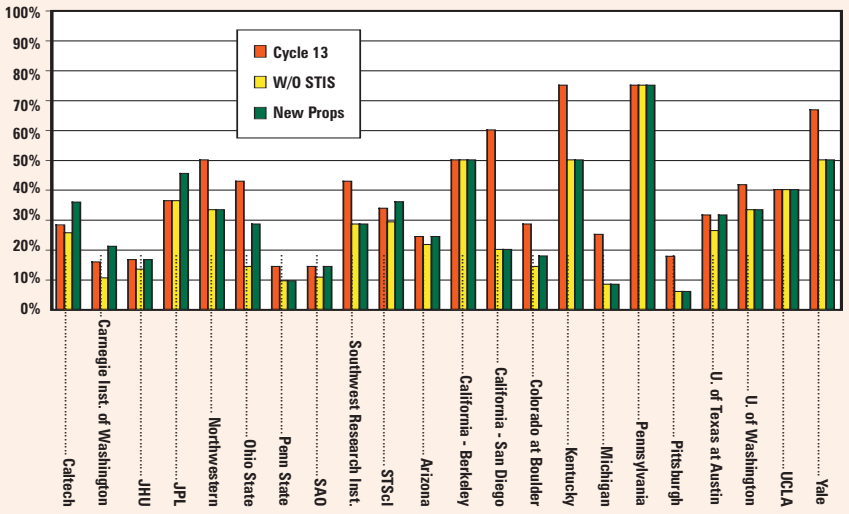


**Figure 2:** Acceptance rates of submitted proposals for the 22 institutions receiving the largest awards of telescope time. Includes the original Cycle 13 allocation (orange), the result with the STIS programs removed (yellow), and the final acceptance rate, after the allocation of STIS replacement programs (green).

### Plans for STIS programs

We notified the PIs of the unexecuted STIS programs in early September that STIS was inoperable and that their programs as proposed would have to be dropped. In all, there were 120 STIS programs from Cycles 11, 12, and 13 that had not been executed. For a handful of these, the PIs could switch to another instrument, maintaining the same scientific method and goals. The vast majority of programs could not be restructured in a way consistent with the criteria by which the Telescope Allocation Committee (TAC) recommended them for selection, and these programs have been dropped from the schedule.

Consistent with our long-standing policy to begin funding for *Hubble* programs only when the first data are available for analysis, the unexecuted programs will not be eligible for funding. Those funds are needed to support the programs activated to fill in the rest of Cycle 13 using the other *Hubble* instruments. Programs that use multiple instruments including STIS may receive a reduction in total funding to reflect the smaller workload, if the program can still be executed returning essential data using the other instruments. The Institute's Grants Office will inform the PIs of the status of their grants.

The TAC evaluation and ranking process has already provided a peer-reviewed list of additional programs that can be scheduled to substitute

*Continued page 4*

STIS Situation
from page 3

for the programs dropped from the schedule. Since each panel, as well as the Cycle 13 TAC, had also ranked programs below the selection cutoff, we used those rankings to select additional programs for scheduling.

We used the absolute rating (rating scale 1.00–5.00, with 1.00 being the top rank) for each program to create a prioritized list of all programs. We eliminated programs that could not be scheduled for technical reasons (for example, those requiring STIS and those that could only be scheduled in early part of this cycle), and selected 2 large, 1 Treasury, and 42 medium and small programs, requiring a total of 1143 orbits. These programs make up the newly-selected program for Cycle 13 scheduling. The TAC itself, as well as the chairs of the Space Telescope Institute Council and the Space Telescope Users Committee, approved this approach. Figures 1–3 summarize the changes.

In all but a few cases, the newly selected programs were in the upper quartile of the original TAC-ranked list. These programs are excellent by the criteria used for selection, and the new Cycle 13 observations contain only the very best science. The demand for *Hubble* time is so great that we can accept only one in six proposals—only a small fraction of the scientifically meritorious projects. Although the loss of STIS is unfortunate, the remaining instruments allow us to maintain the scientific output at the highest level.

We will notify the newly-selected observers, who will have four weeks to develop Phase II programs and submit budget requests. New programs will be added to the long-range plan of observations as soon as possible after they are submitted.

We appreciate the difficulty that the loss of STIS will cause for many scientific groups around the world, and we are sorry to bring you this bad news. However, the project engineers are also looking carefully at potential ways to restore the instrument, and we will keep you informed of any progress that is made. Ω

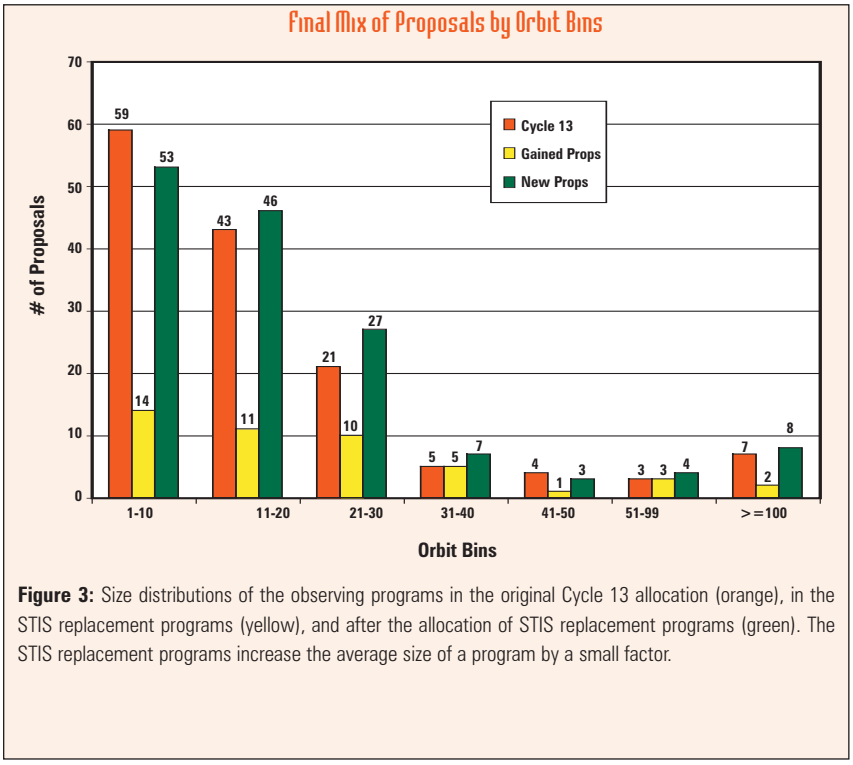


**Figure 3:** Size distributions of the observing programs in the original Cycle 13 allocation (orange), in the STIS replacement programs (yellow), and after the allocation of STIS replacement programs (green). The STIS replacement programs increase the average size of a program by a small factor.

*Old Stellar Systems from page 1*

### Products for the community

We have already obtained mid-UV echelle spectra with the Space Telescope Imaging Spectrograph (STIS) for individual stars all across the color-magnitude diagram, including red giants, blue stragglers, turnoff stars, and extreme blue horizontal branch stars. All our data are made public as soon as they are taken and archived by the Multi-mission Archive at Space Telescope (MAST) at **http://archive.stsci.edu**.

Our unique contribution and 90% of our effort is to provide theoretical spectral calculations of stars and of simple composite stellar systems. Unlike empirical templates, our theoretical calculations can span the entire range of stellar temperature, metallicity, and elemental abundance ratios that are found in old systems. Our calculations yield fluxes at high resolution, which can be smoothed to match those of any observed spectrum and can be integrated to form spectral indices and broad-band colors.

Our program is less than half complete observationally. We have obtained enough STIS echelle spectra to ensure our calculations can eventually match solar-metallicity stars. However, we have obtained only one of our metal-rich field stars and none of our cluster stars. The latter include the stars in the rectangle in the cluster pictured in Figure 1, the metal-rich old open cluster NGC 6791. Like those in luminous galaxies, stars in this cluster have enhanced sodium and magnesium line strengths. Moreover, the cluster harbors hot blue stars (circled), which are believed responsible for the upturn in UV flux seen in many luminous elliptical galaxies.

Should STIS not recover, we have requested lower-resolution spectra of these stars and imaging of the M31 clusters by the Advanced Camera for Surveys (ACS) in the mid-UV, near-UV, and optical bands. This will ensure that we can check our stellar calculations at metallicities above solar and can confirm our isochrone-based co-addition weights at and above solar metallicity for systems with enhanced light-element abundances.

Our theoretical program is only about 10% complete. We are first comparing our calculations to STIS echelle spectra that we have just taken for individual standard stars. We will soon calculate grids of theoretical spectra for all these types of stars over a wide range of metallicity. We will construct separate grids for the solar mix of abundances and for mixes with enhanced light elements. We will then generate theoretical spectral templates for single-age, single-metallicity systems by co-adding the stellar spectra with weights derived from the isochrones, which we are calculating for these same metallicities and mixtures. We will distribute our atlases comparing theoretical spectra to our STIS echelle observations, as are shown in Figures 8–11 below. The MAST archive has generously agreed to host these atlases and to be the repository of our theoretical stellar and composite grids.

With proper calibration, our public theoretical products can include colors for both space-based and ground-based photometric systems. We anticipate generating grids of colors for single-age, single-metallicity populations as functions of age, metallicity, light-element enhancement, and reddening, for ourselves and others to combine for interpreting remote galaxies. These colors will be included as part of our MAST archive products.

### Standard stars

To improve the calculations and ensure their validity, we first match our spectral calculations to real spectra of standard stars. As described by R.C. Peterson, B. Dorman, & R.T. Rood (2001, *ApJ*, 559, 372), we change input atomic-line parameters, then recalculate all standard stellar spectra, iterating until a satisfactory match is achieved for all stars simultaneously. Many lines are "missing" from the calculations because they have not been detected in the laboratory; we manually add these as lines of Fe**I**. Assuming local thermal equilibrium (LTE), and adopting new models from F. Castelli and R.L. Kurucz (2003, IAU Symp. No. 210, *Modeling of Stellar Atmospheres*, eds. N. Piskunov, et al., CD-ROM poster A20; astro-ph/0405087; available as ODFNEW from **http://kurucz.harvard.edu/grids/**), we get good fits for mildly weak-lined stars, as shown in Figures 8–11. We still must improve the fits to the Sun, using existing STIS spectra of strong-lined and hotter stars.

As we fit the standards, we must redetermine their own parameters. We demand matches for all stars in the profiles of strong lines and H-alpha (Figures 2–3) as well as in the weak-line strengths (Figures 4–7) and in mid-UV flux and line strengths (Figures 8–11). Our Arcturus and Procyon (HD 61421) values determined in this way agree well with other recent results.

### Plots showing goodness of fit

In Figures 2 through 11, we compare the theoretical spectra (light black line) with observations (heavy black line) using the atlases of Kurucz et al.

*Continued page 6*

**Figure 1 (Cover Image)**

The old open cluster NGC 6791, a Milky Way surrogate for metal-rich extragalactic stellar systems. The figure is derived from multicolor imaging, with *B-V* colors enhanced to the blue and *V-I* colors enhanced to the red to highlight its extremely old, hot cluster members (circled), which are as blue as the young, bright blue field interlopers. Hot blue members are present despite the fact that the cluster metallicity is a factor of two greater than solar. They are of the subdwarf O/B type believed to cause the upturn seen in ultraviolet fluxes of luminous ellipticals. The cluster also harbors blue stragglers just above the main-sequence turnoff. One of these, and two nearby turnoff stars, are seen inside the rectangle; these are our three targets for spectroscopy to confirm our mid-UV line-strength calculations in turnoff stars at high metallicity. Figure courtesy of E.M. Green.

*Old Stellar Systems from page 5*

(1984, NSO Publ. No. 1) for the Sun, Hinkle et al. (2000, *Visible and Near Infrared Atlas of the Arcturus Spectrum*, K. Hinkle, L. Wallace, J. Valenti, & D. Harmer, ASP) for Arcturus, and Texas, Lick, and STIS echelle spectra for the rest. In the mid-UV, a single flux normalization constant is adopted at all wavelengths. Procyon's constant is 8.5% larger than that implied by its angular diameter, marginally consistent with the current accuracy of STIS spectroscopic fluxes.

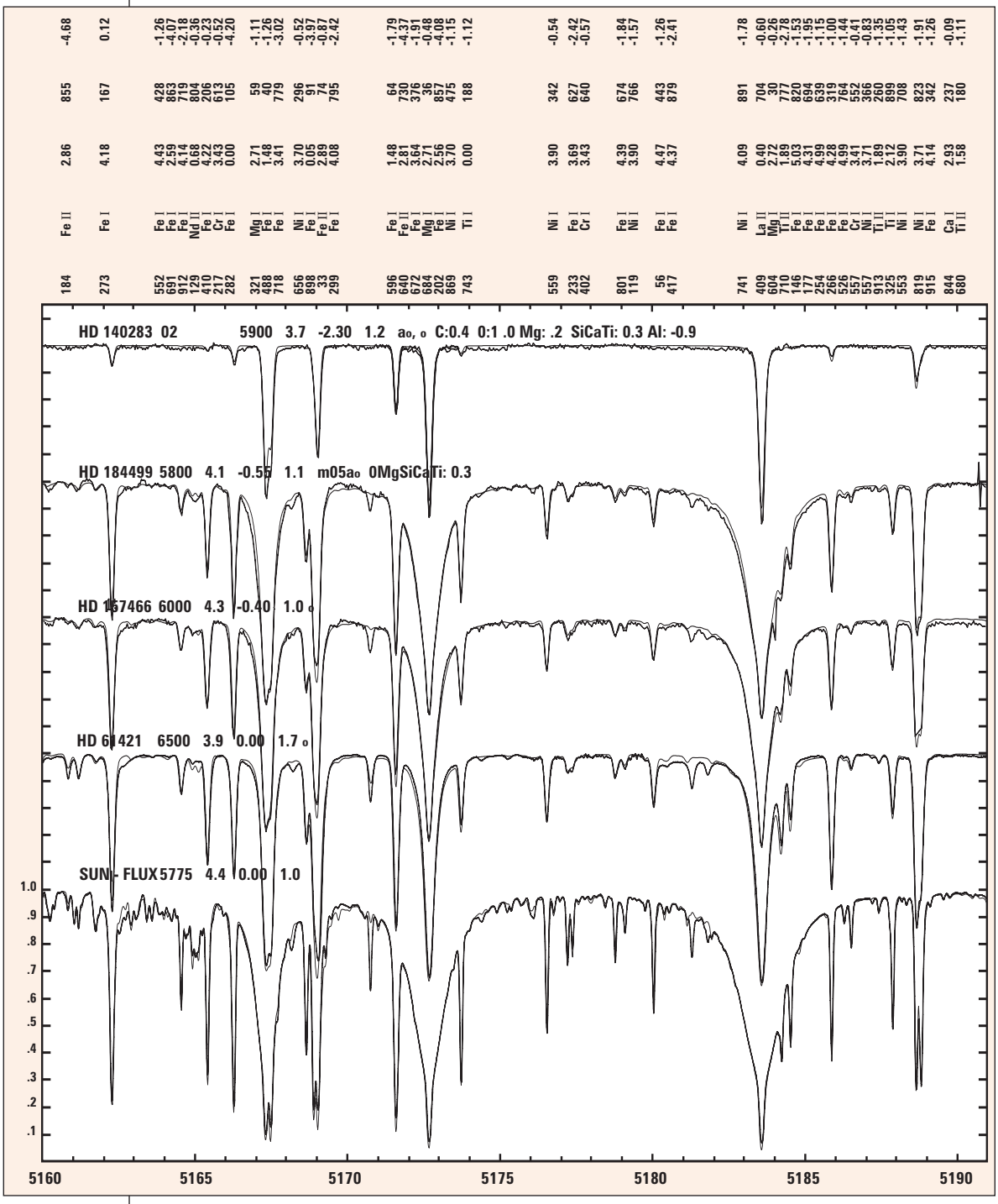


**Figure 2**

### Stellar parameters

Metallicity is found from weak lines such as FeI 4604.557 Å, as seen in Figures 4–7. Temperature is assessed by matching H-α (Figure 2) and from high vs. low FeI lines such as 4602.001 Å. Many are strong, so microturbulent velocity must be derived by comparing strong and weak FeI lines such as 4602.001 Å and 4602.901 Å with furnace *gf* values (for references see Blackwell, D.E., Lynas-Gray, A.E., & Smith, G. 1995, *A&A*, 296, 217). Gravity is from FeII lines such as 4620.521 Å, as well as from profiles of strong lines (Figures 3, 8–11). UV flux must also match. While it does so reasonably well for all stars shown in Figures 8–11, temperature changes up to 50 K might still be needed: higher for Procyon, lower for HD 184499.

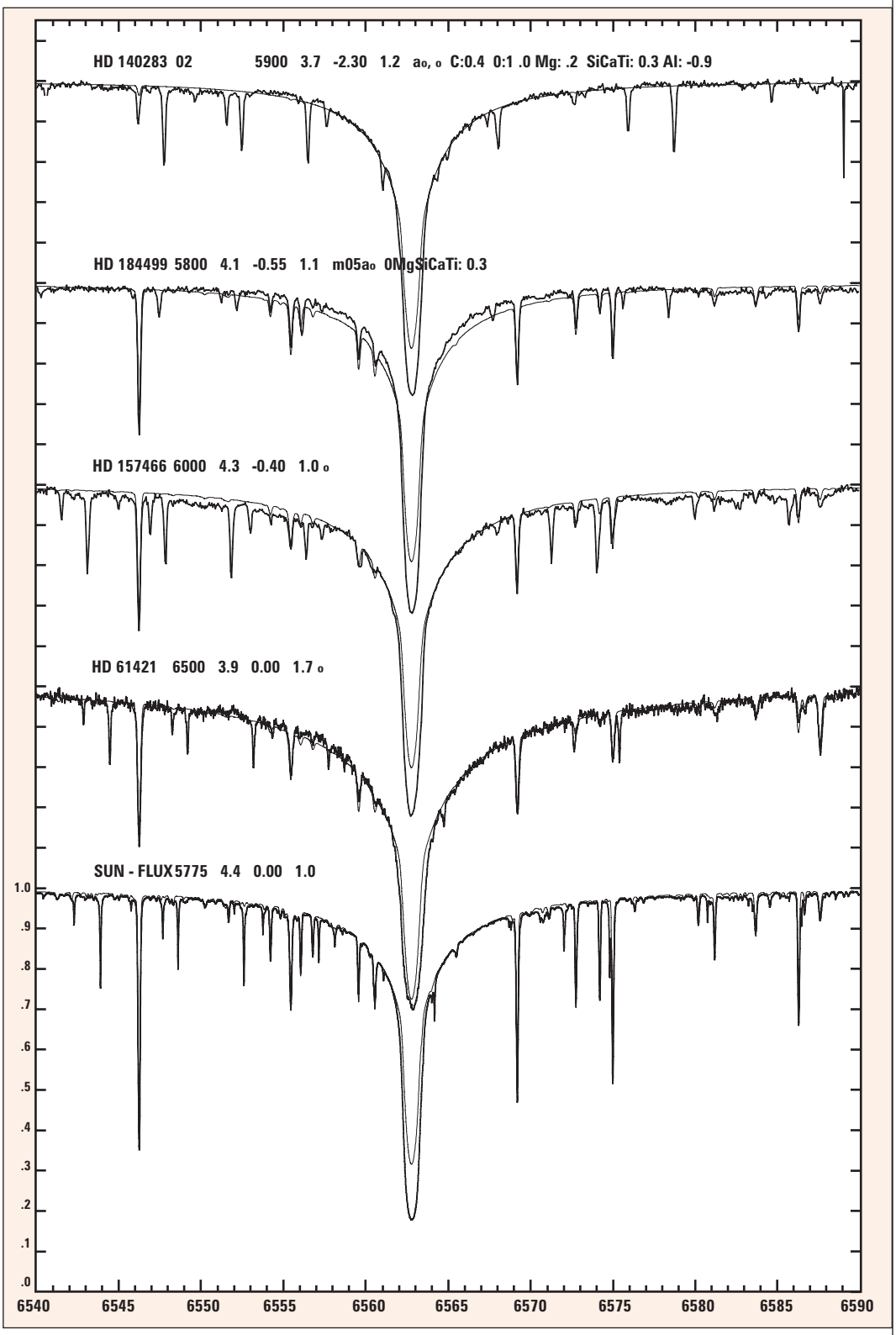


**Figure 2–11**

Plots are shown comparing our theoretical spectra (light black line) with observational echelle spectra (heavy black line). In color appear theoretical calculations for a single element only, from Mn and Co (yellow) to the heaviest elements (purple and blue). Wavelength in Å appears at the bottom, and Y-axis ticks represent 10% of the full scale. Stars are offset for visibility; the Sun is at the bottom, and Procyon is listed as HD 61421. Identifications for the strongest lines appear at the top. The values are (1) the decimal digits of the wavelength in Å, (2) a colon if it is a "missing" FeI line, (3) the species and its excitation potential in electron volts (or band), (4) the residual intensity in the solar or Arcturus spectrum, and (5) the log *gf* value.

Next to each star's name are best-fit model parameters $T_{eff}$, log *g*, [Fe/H] (log of the stellar-to-solar iron abundance ratio), and microturbulent velocity in km/s. These are followed by the relative abundances of elements showing deviations from solar. [X/Fe] is the log of the stellar-to-solar ratio of the abundance of element X with respect to iron; [X/Fe] = –0.3 is a factor-of-two deficiency.

**Figure 3**

*Continued page 8*

*Old Stellar Systems from page 7*

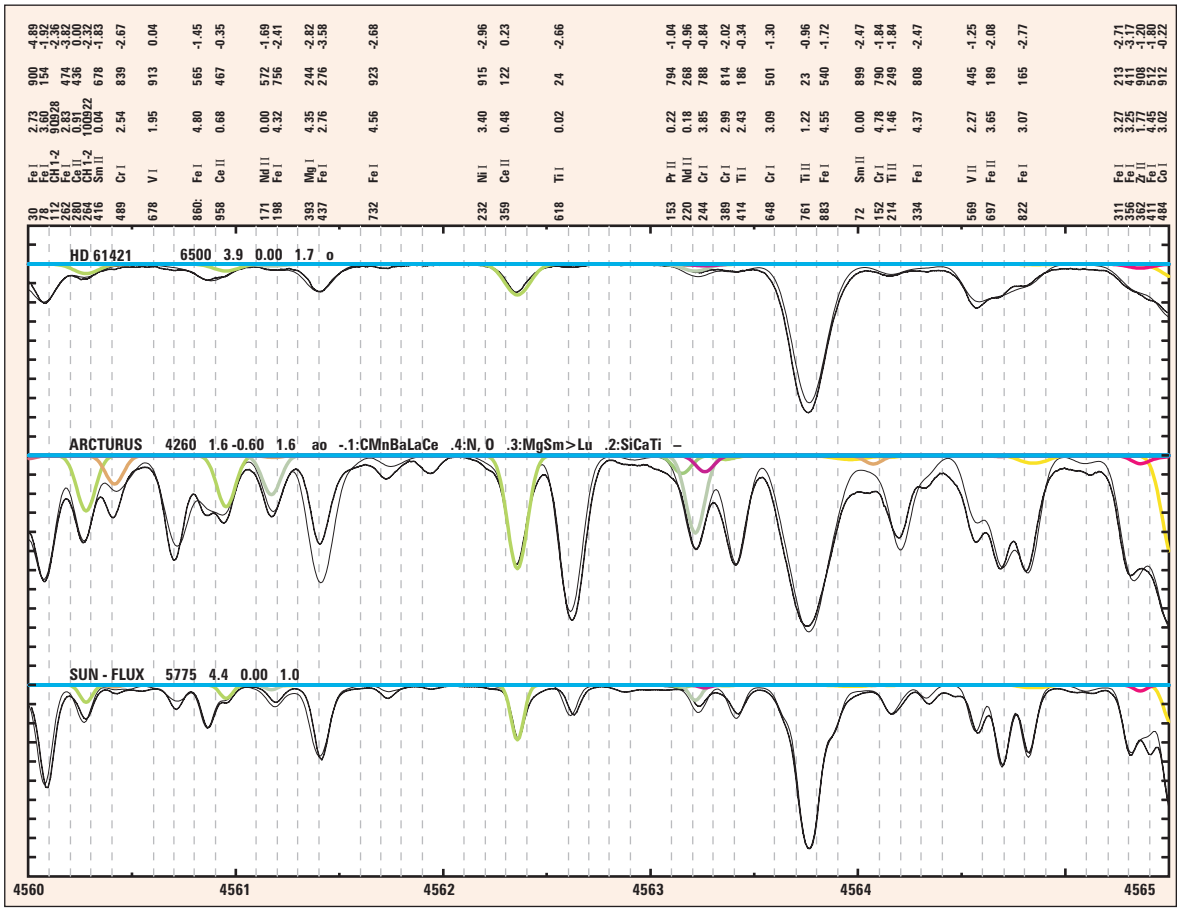


Figure 4

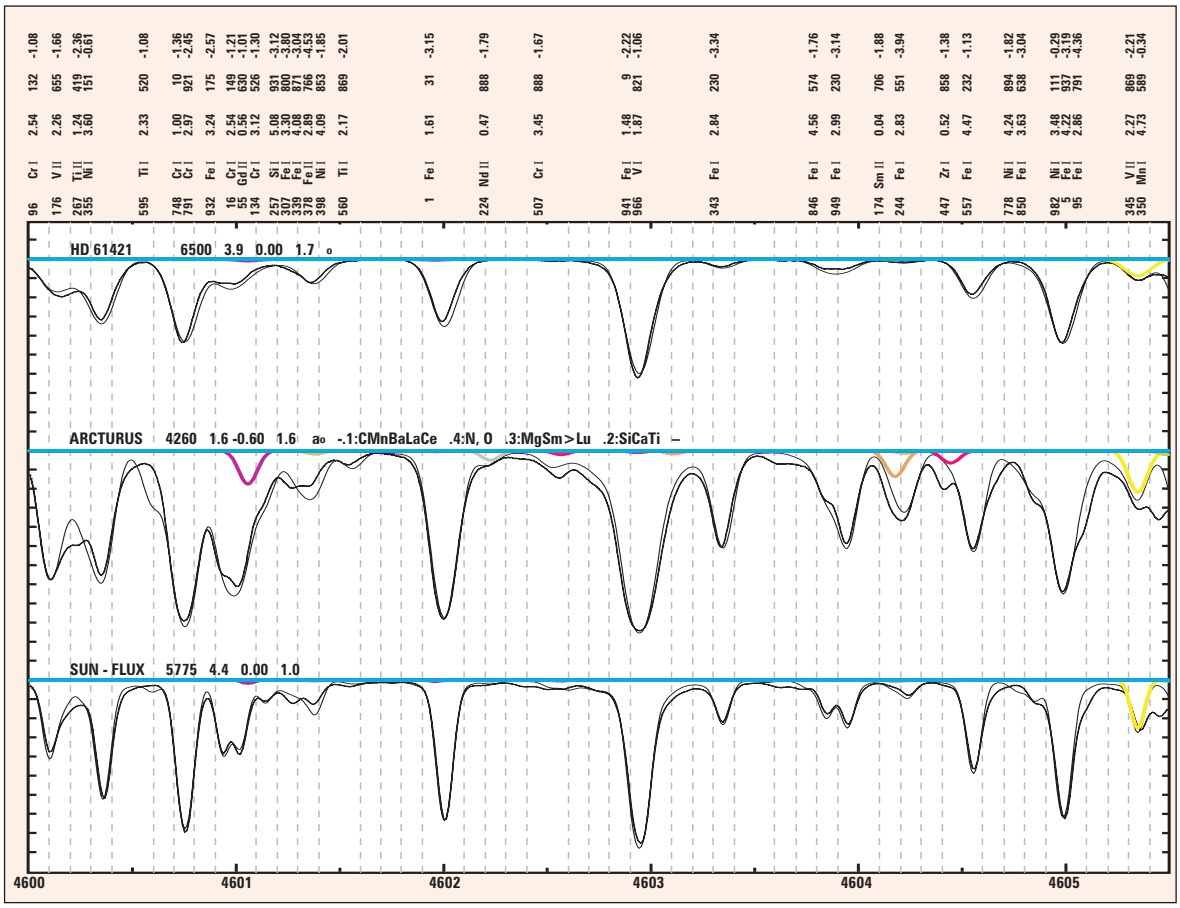


Figure 5

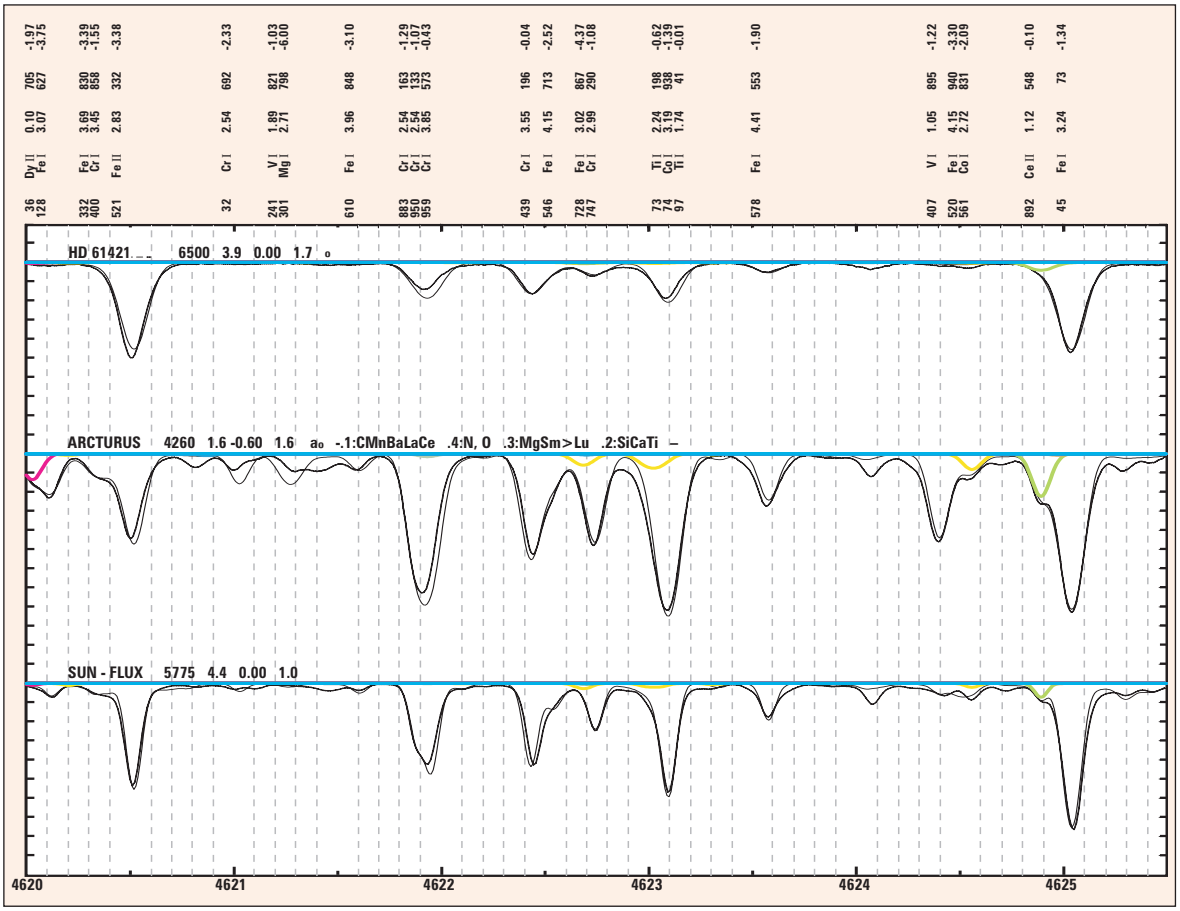


Figure 6

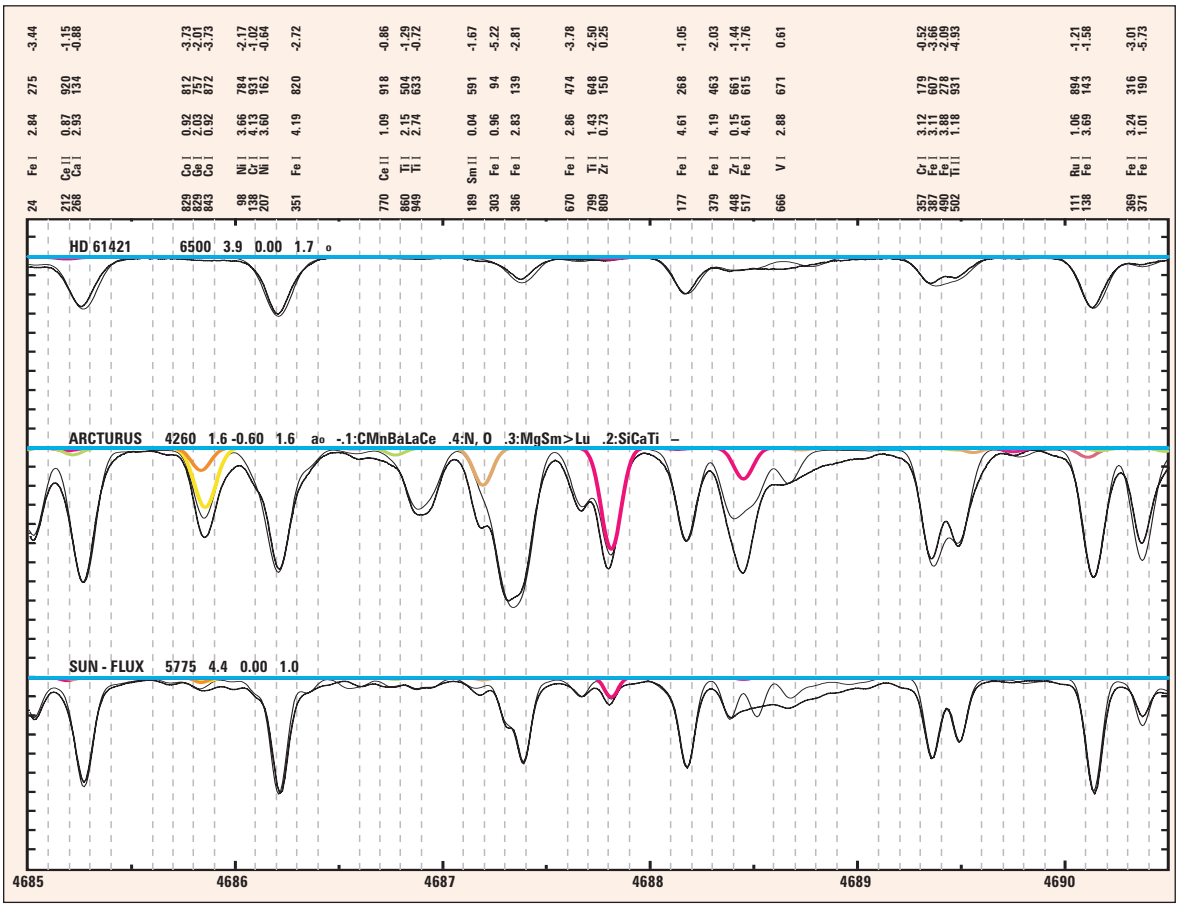


Figure 7

*Old Stellar Systems from page 9*

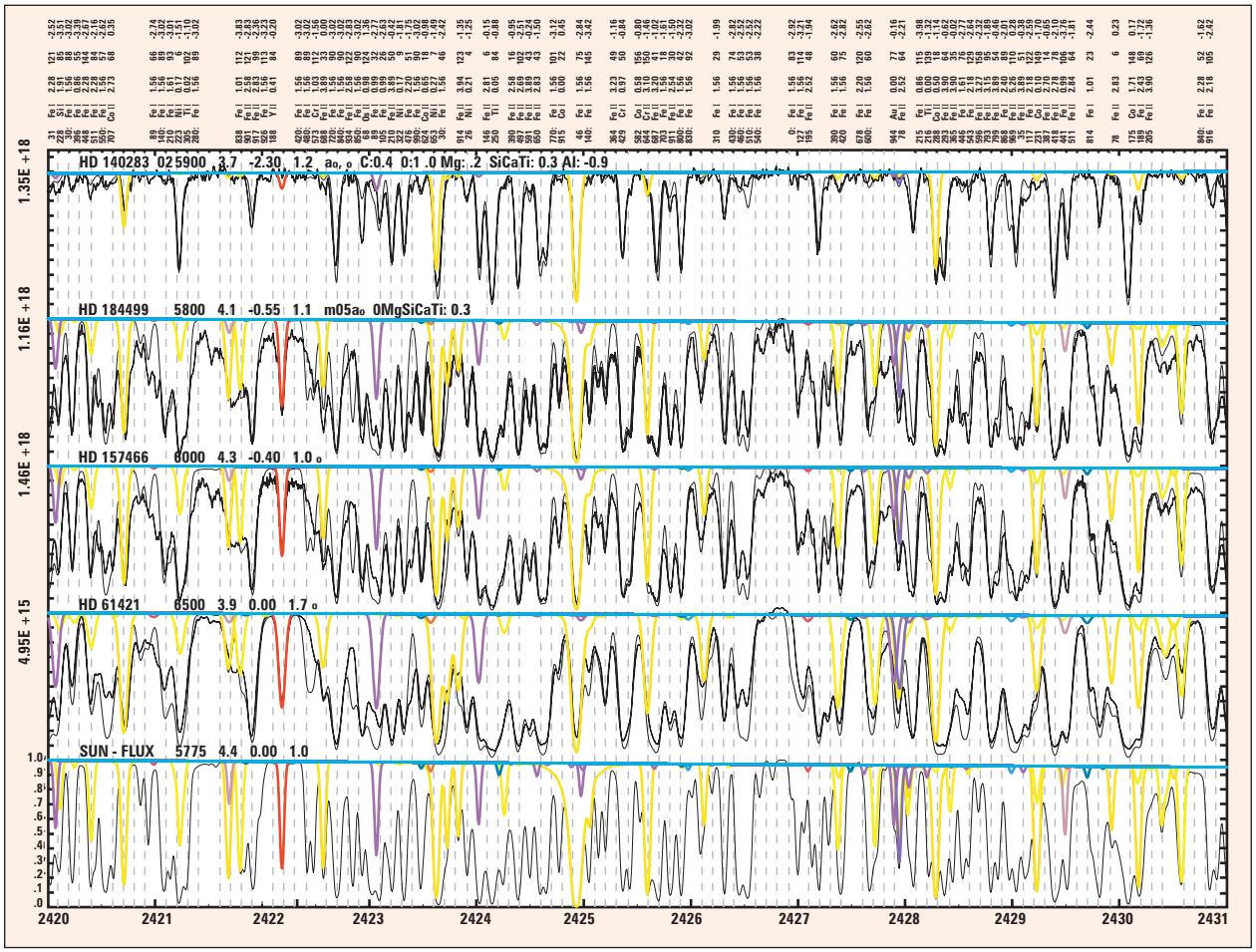


Figure 8

Figure 9

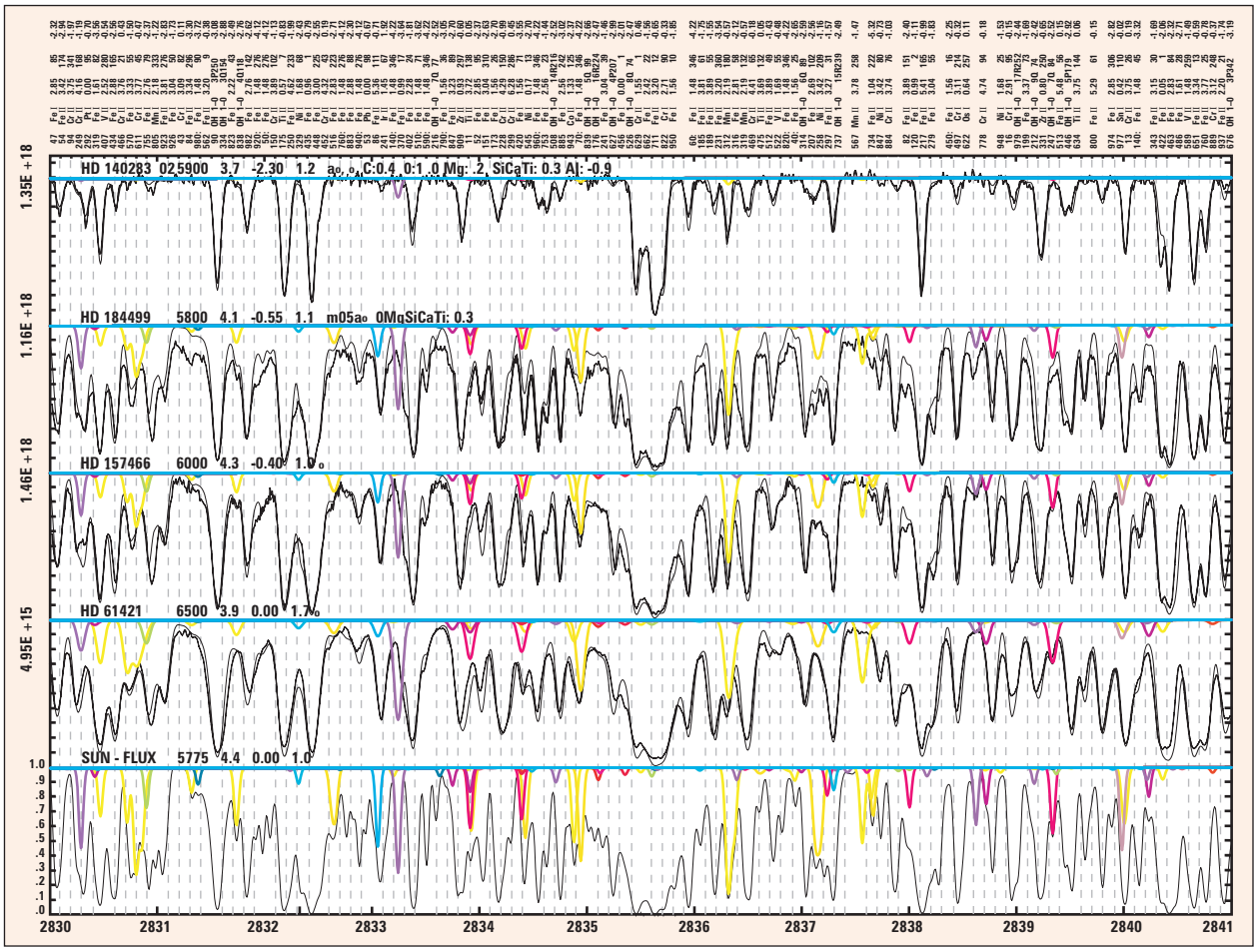

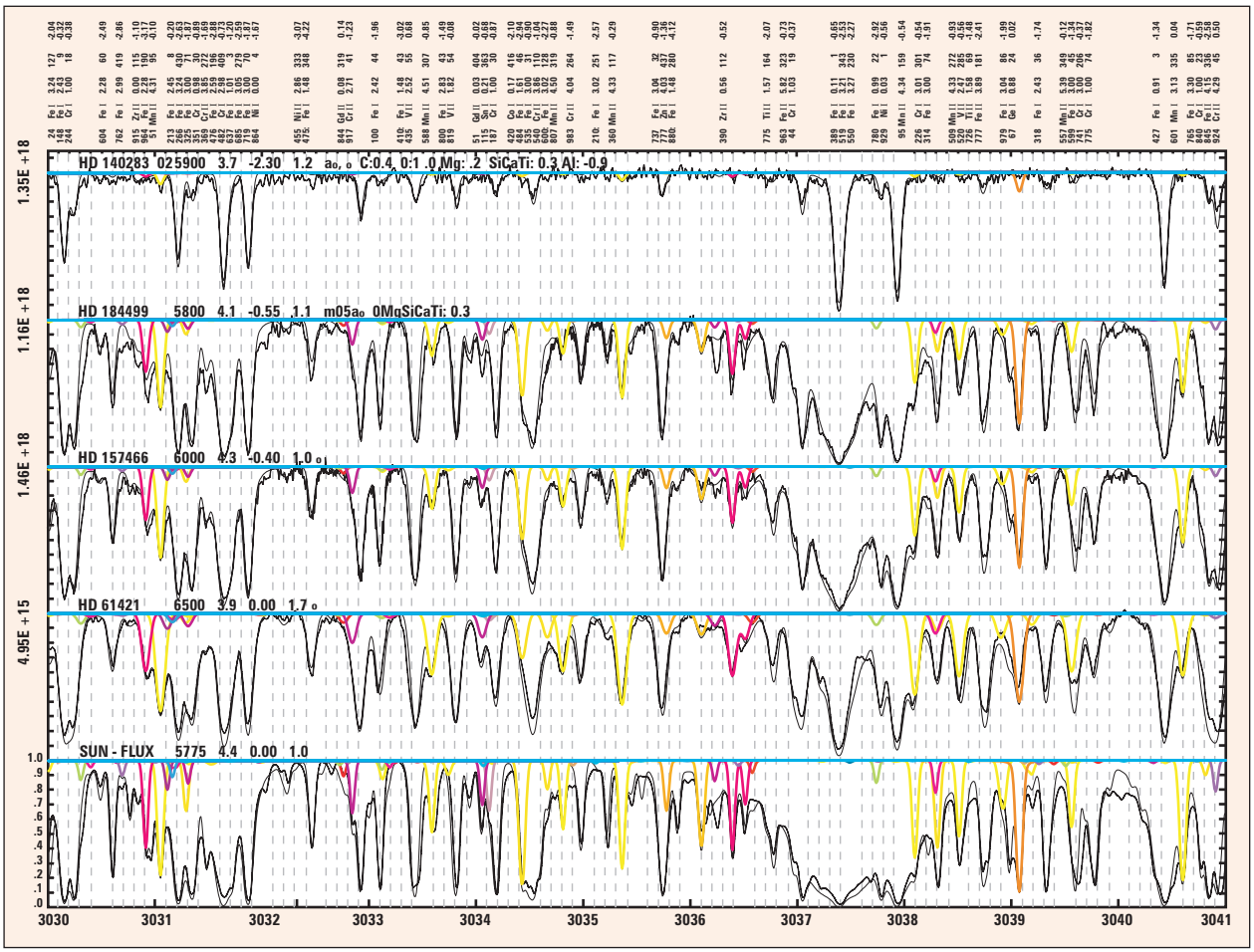


Figure 10

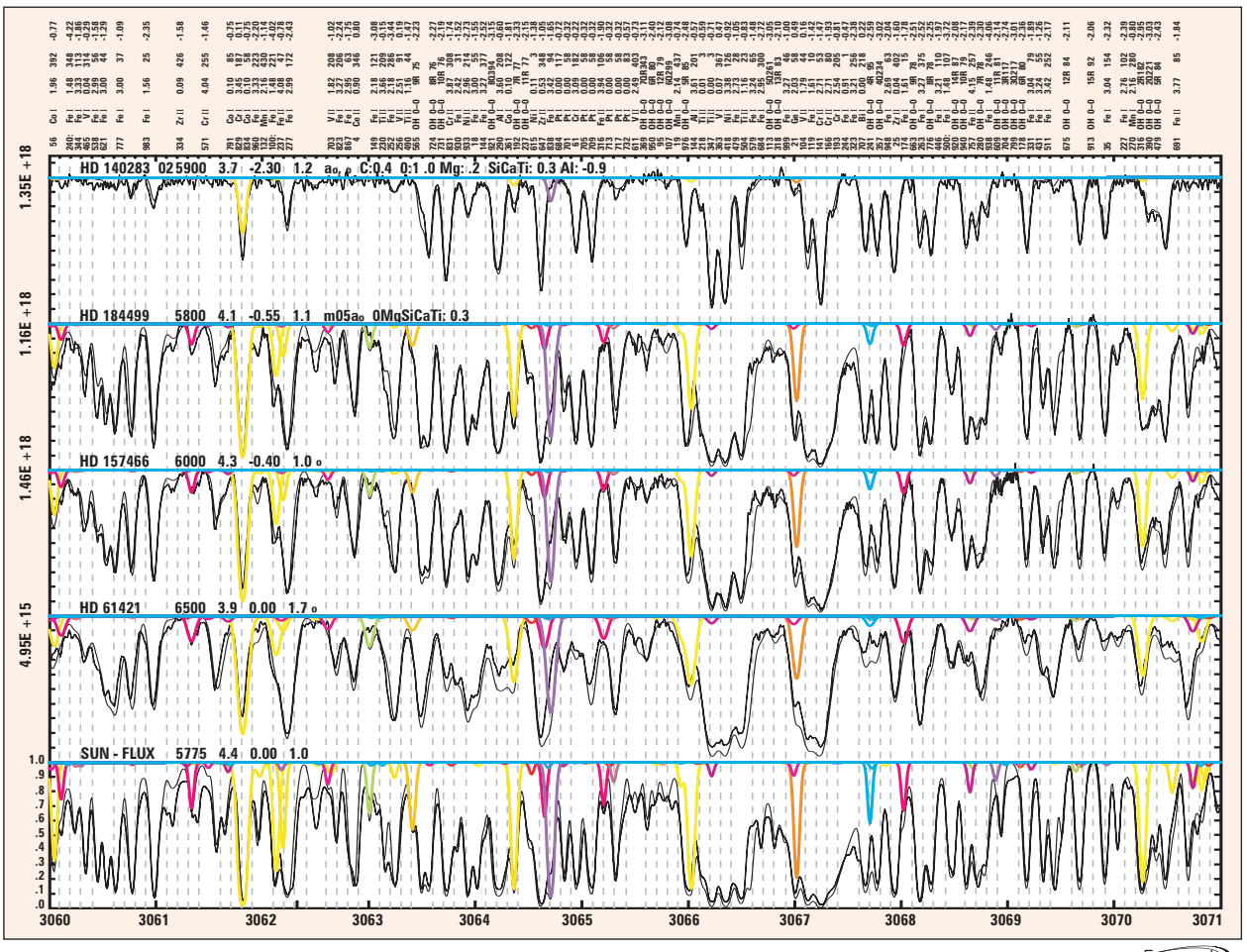


Figure 11

*Old Stellar Systems from page 11*

### Determining abundances of rare earth elements

One consequence of our spectral fits to standards is the ability to refine abundance determinations. This is important, especially for very light and very heavy elements with few accessible lines.

In the blue and mid-UV plots in Figures 4–11, theoretical spectra including only lines of a given heavy element appear in color, resulting in a solid blue line at 100% intensity. Yellow is Mn ($Z=25$) and Co (27), red Y (39) and Zr (40), green La (57) and Ce (58), and purple to blue, increasingly heavier elements. This match required lowering the solar Zr abundance by about 0.1 dex. In Arcturus, Y and Zr were found to be relatively deficient and the purple heavy *r*-process elements such as Eu relatively enhanced.

Abundances of many rare-earth elements can be found from the optical, such as that of cerium from CeII 4562.359 Å and other lines. Some elements are best measured from the mid-UV, however. Germanium, for example, does have optical lines, but like GeI 4685.829 Å, these are generally severely blended even in cool giants like Arcturus. In the mid-UV Ge is potentially detectable even in weak-lined stars. GeI 3039.067 Å matches in the Sun and two of the three metal-poor stars, but is too strong in Procyon and in HD 140283. Its relative abundance apparently varies from star to star. However, lines of GdII 3032.844 Å and 3034.051 Å both match all stars. ZrII lines like 3036.390 Å match as well in the mid-UV as in the optical.

Some species with poorly determined abundances have lines in the mid-UV that will require more effort to disentangle them from their neighbors: SnI at 3034.115 Å, for example. Other species sometimes are consistently mismatched, like PtI 3064.684 Å and IrII 2833.241 Å. We continually need to update *gf* values.

We need improved hyperfine splitting as well. It has been included for most odd-*Z* elements, but is still lacking for several critical elements and occasionally erroneous in abundant elements such as cobalt and manganese, which are ubiquitous mid-UV absorbers.

### Application to M31 globular clusters and external galaxies

Our calculations have already been applied to globular clusters. Rather than compare against a theoretical spectrum of an individual star, we generate a composite spectrum representing a single-age, single-metallicity population. We do this by co-adding individual stellar spectra representing stars at strategic places along the appropriate color-magnitude diagram. We will construct weights for co-addition of these spectra by calculating stellar tracks of the same metallicity and light-element-to-iron ratio as for the theoretical spectra. We plan to include tracks in which oxygen alone is enhanced, as well as the solar mix and ones with Mg, Si, Ca, and Ti enhancements.

In R.C. Peterson et al. (2003, *ApJ*, 588, 299), we applied a simplified version of composite spectra to archival optical and mid-UV spectra of the mildly metal-poor M31 globular cluster G1. We adopted weights derived from the color-magnitude diagram of the Milky Way globular 47 Tucanae, of similar metallicity. We obtained very good fits to the spectra in both wavelength regions, but only when theoretical spectra from hot stars such as those circled in Figure 1 were included. Both cool and hot horizontal-branch stars were needed; blue stragglers gave poorer fits. We found for G1 a metallicity [Fe/H] = –0.8 as inferred from the giant branch, and an age comparable to that of halo stars in our galaxy. Ω

## Majestic Cousin of the Milky Way

Like our Milky Way, this galaxy has a blue disk of young stars peppered with bright pink star-birth regions. In contrast to the blue disk, the bright central bulge is made up of mostly older, redder stars.

NGC 3949 lies about 50 million light-years from Earth. It is a member of a loose cluster of some six or seven dozens of galaxies located in the direction of the Big Dipper, in the constellation Ursa Major (the Great Bear).

**http://hubblesite.org/newscenter/newsdesk/archive/releases/2004/25/**

***Image Credit:*** NASA, ESA, and The Hubble Heritage Team (AURA/STScI)

# Advanced Camera for Surveys News

**R. Gilliland,** *gillil@stsci.edu*

The Advanced Camera for Surveys (ACS) continues to provide scintillating results from imaging of objects ranging from our own solar-system neighbors to galaxies at the edge of the universe.

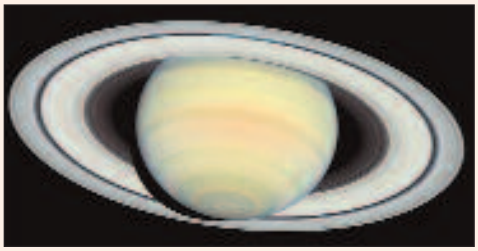

**Figure 1:** Saturn as viewed with the ACS High Resolution Camera (HRC) in March 2004.

In a complementary role to NASA's current flagship planetary mission, *Hubble,* imaging with the High Resolution Camera of the Advanced Camera for Surveys (ACS), has provided Saturn monitoring from a perspective different from that of *Cassini* as it closed in on its target.[1] Eric Karkoschka and his team observed Saturn this spring both from near-Earth with *Hubble* and from *Cassini* as it hurtled toward its successful rendezvous with the ringed planet last summer. This provided the first chance for astronomers to compare views of Saturn with near-equal sharpness from two very different perspectives. Now that *Cassini* is resident at Saturn, its resolution will surpass that provided by the remote *Hubble*. Nevertheless, continued collaborations between these two grand observatories will provide unique science based on stereoscopic views.

A team led by Andrew Gould, David Bennett, and David Alves has used observations with the Wide Field and Planetary Camera 2 (WFPC2) in 1999 and ACS in 2002 and 2003 to split the lens and source stars from a microlensing event discovered in 1993 from Australia.[2] Separating the two stars allowed determination of the lensing star parallax. As the distance is known to the Large Magellanic Cloud (LMC), where the source resides, the only remaining unknown in matching the microlensing light curve is the mass of the lens, which could now be fixed. The foreground star turns out to have a mass of one-tenth that of the Sun, and is thus a common (but not that easy to see) low-mass M dwarf. The high angular resolution provided by *Hubble* was key to this first (gravitational) determination for the mass of a single star.

The continuing, unique, narrowband filter capability of the WFPC2 is showcased in a Hubble Heritage image of N11B, the second largest star-forming region (after 30 Doradus/Tarantula nebula) in the LMC.[3] The science team led by You-Hua Chu and Yäel Nazé is comparing these images of N11B, taken in 1999, with similar regions elsewhere in the LMC in a study of sequential star formation.

**Figure 2:** A WFPC2 view of the LMC N11B nebula based on a color composite of F502N ([OIII]) and F656N (H-alpha) filters.

John Blakeslee and Holland Ford led a science team exploiting parallel observations with the ACS Wide Field Camera (WFC) to showcase what turns up in a typical patch of sky.[4] In this case, the composite image (from a total of 40 hours including F435W (*B*), F606W (*V*), F775W (*I*), and F850LP (*z*) images) shows a particularly dramatic blue arc associated with the red galaxy at image center. Follow-up spectroscopy has provided a firm redshift of 0.6 for the lens, and a photometric redshift of 2.4 follows for the arc. Studies such as this provide a means of directly assessing the mass of ordinary, moderate-to-high-redshift galaxies.

[1] http://hubblesite.org/newscenter/newsdesk/archive/releases/2004/18
[2] http://hubblesite.org/newscenter/newsdesk/archive/releases/2004/24
[3] http://hubblesite.org/newscenter/newsdesk/archive/releases/2004/22
[4] http://hubblesite.org/newscenter/newsdesk/archive/releases/2004/21

*Continued page 14*

ACS from page 13

Of particular note for community science support, the ACS group at the Institute has released Version 3.0 of the *ACS Data Handbook*, edited by a team led by Cheryl Pavlovsky and Jennifer Mack. New to this version are fully up-to-date discussions of what has been learned from two years of scientific use and calibration of ACS. The new Chapter 5 quantifies error sources, including readout noise, flat field properties, and cosmic rays, which adversely (but quite naturally) affect ACS data. Chapter 6 on ACS data analysis provides a guide to extracting information for photometry, astrometry, polarimetry, coronagraphy, ramp filters, and grism/prism spectroscopy. The *ACS Data Handbook* is available in various formats from **http://www.stsci.edu/hst/acs/documents** and now provides the complete set of information needed for users to analyze and interpret their data.

**Figure 3:** An eclectic mix of galaxies observed in a parallel, random-field, observation with the Wide Field Camera of ACS. Of particular science interest in this case is the dramatic blue arc from gravitational lensing of a distant galaxy by the foreground red galaxy.

Three Instrument Science Reports (ISRs) written by John Biretta and Vera Kozhurina-Platais document significant advances in our understanding of polarimetric calibration for the ACS. They can be found at **http://www.stsci.edu/hst/acs/documents/isrs**. ACS ISR 04-09 introduces the issues and reviews the range of existing ground-based test information and on-orbit calibration data. ACS ISR 04-10 discusses a novel determination of the POLV filter angles by noting that the residual positions of stars between polarized and unpolarized observations are anisotropic and rotate modulo the orientations of the polarizer filters. This has confirmed the proper mounting of filters and provides an independent measure in detail of these critical angles. ACS ISR 04-11 provides detailed quantification of the unique geometric distortions introduced with the ACS/HRC polarimetric filters; the new solutions are good to better than 0.03 pixels. Polarimetry, always an undertaking requiring extra care and calibrations, will continue to see enhancements in the future as further special calibration observations are obtained and analyzed.

Two ISRs by Mauro Giavalisco provide analyses of minor cross-talk effects in the four amplifiers of the WFC. ACS ISR 04-12 provides a description of the effect along with examples. Generally, a bright object in one quadrant leads to minor, additive (negative) offsets at a mirror-symmetric position in the other quadrants. The effect is generally only a cosmetic issue, involving a few electrons per pixel, and it would often be corrected by local background subtraction. ACS ISR 04-13 provides analyses of data taken with the non-default GAIN = 2 e-/DN value. It concludes that the ghost images are generally much smaller than with GAIN = 1, thus arguing that those wishing to avoid such cosmetic effects should select GAIN = 2.

With the likely loss of the Space Telescope Imaging Spectrograph, the importance of the ACS Solar Blind Channel (SBC) will rise dramatically. The SBC uses a Multi-Anode Microchannel Array (MAMA) detector in the far ultraviolet (FUV), with heritage from the STIS/FUV detector development. One of the rationales for including the SBC on ACS was to provide a partial backup for the low-noise, FUV capability of STIS. The ACS/SBC has been little used, possibly less than actually warranted by a straightforward consideration of its capabilities relative to the far more heavily used STIS/FUV. Of course, the latter had spectroscopic options far beyond the small range offered by the prisms of the ACS/SBC. For example, in Cycle 13 only 6 orbits for imaging and 7 for spectroscopy with the SBC were approved, which is less than 1% of the overall ACS allocation. Cycle 13 STIS/FUV allocations were 18 imaging and 532 spectroscopic orbits, or 5% of the total STIS use. The ACS group at the Institute and our colleagues at the Space Telescope European Coordinating Facility, who conducted the primary calibrations for ACS prism and grism spectroscopy, will strive to ensure that the ACS/SBC can be utilized as fully as possible to cover the unique science in the FUV.

A recent study of the ACS/SBC dark current by Colin Cox has been released as ACS ISR 04-14. A primary finding is that the dark current realized in normal operations is about $1.0 \times 10^{-5}$ counts per pixel per second, a factor of four smaller than that in the reference dark that was in place, and 20% smaller than the general dark noise in the Exposure Time Calculator (ETC) and the *ACS Instrument Handbook*. Updated values are now in place in the ETC and handbook. Ω

# NIRSpec Enters Implementation Phase

**P. Jakobsen,** *pjakobsen@rssd.esa.int*

The near-infrared spectrograph (NIRSpec) of the *James Webb Space Telescope* (*JWST*) has recently passed two major milestones. The European Space Agency (ESA) selected EADS Astrium GmbH in Ottobrunn, Germany, as the prime contractor for the construction of NIRSpec and appointed the flight Instrument Science Team (IST) for the instrument.

ESA will provide NIRSpec with ESA funds, and European industry will build it under ESA project supervision. NASA will provide two key components, the slit selection device, which uses Microelectromechanical System (MEMS) technology, and the near-infrared detector array. Together with the Optics Module of the Mid-Infrared Instrument, NIRSpec constitutes Europe's instrumental contribution to the *JWST* mission.

The NIRSpec instrument has been the subject of competitive industrial assessment and definition studies since 1998. Its present, near-final design and capabilities follow closely the recommendations originally made for the instrument by the Ad Hoc Science Working Group (ASWG).

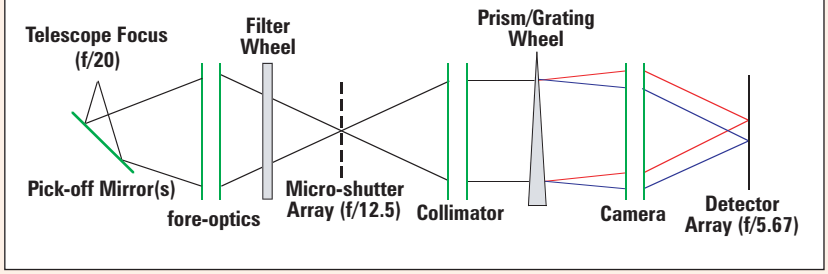


**Figure 1:** Schematic of the NIRSpec optical system.

NIRSpec is a multi-object spectrograph capable of obtaining the near-infrared spectra of 100 or more astronomical sources simultaneously, at a spectral resolution of $R\sim1000$ over the 1 to 5 micron wavelength range or at a spectral resolution of $R\sim100$ over 0.6 to 5 micron. The $R\sim100$ mode employs a single prism as its dispersive element and is intended for measuring the redshifts and continuum spectra of faint galaxies. The $R\sim1000$ mode utilizes three diffraction gratings to cover its range and is primarily intended for detailed follow-up observations using conventional nebular emission lines as astrophysical diagnostics. Lastly, three $R\sim3000$ gratings, also covering 1 to 5 micron, will allow kinematic studies of individual objects in single-object mode, using either a fixed, long slit, or an Integral Field Unit (IFU).

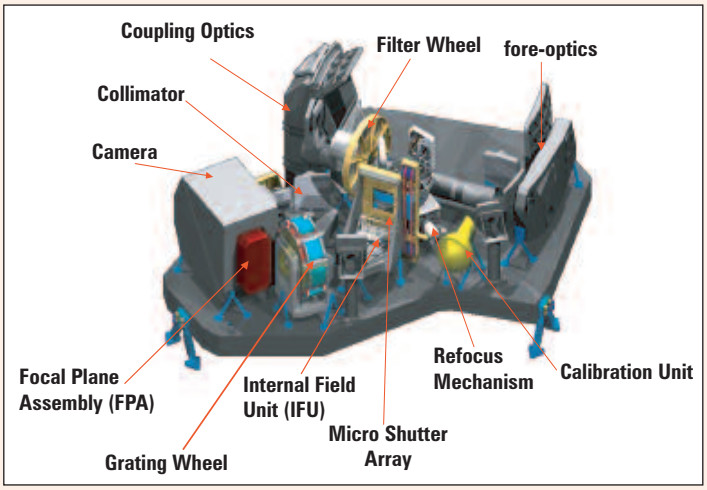


**Figure 2:** Layout of NIRSpec. The instrument measures 190 cm across and weighs close to 200 kg (EADS Astrium).

The Astrium NIRSpec design employs all reflective optics, with most of its optical and structural elements manufactured out of SiC, a ceramic material whose application in cryogenic space optics has been pioneered by the development of the primary mirror for ESA's *Herschel* mission.

While conventional in its optical concept, NIRSpec's large, ~9-arcminute$^2$ field of view and fast *f*-ratio require sophisticated and challenging mirror surfaces to maintain image quality over the full field of view. The NIRSpec optical chain (Figure 1) consists of three main components, which are implemented as three-mirror-anastigmat (TMA) sub-units, which can be individually assembled and tested during integration. The fore-optics re-image and

*Continued page 16*

*JWST NICSpec*
*from page 15*

de-magnify the focal plane image of the *JWST* proper onto the slit-selection mechanism. The collimator converts the light emerging from each slit into a parallel beam and projects it onto the grating wheel, which carries the six (flat) reflective gratings, the (dual-pass, reflective) prism and a flat mirror for target acquisition. The camera finally focuses the dispersed collimated light coming off the grating onto the detector array. A filter wheel, located in the internal pupil of the fore-optics, carries the requisite order-isolation filters for the diffraction gratings and also serves as the instrument shutter (Figure 3).

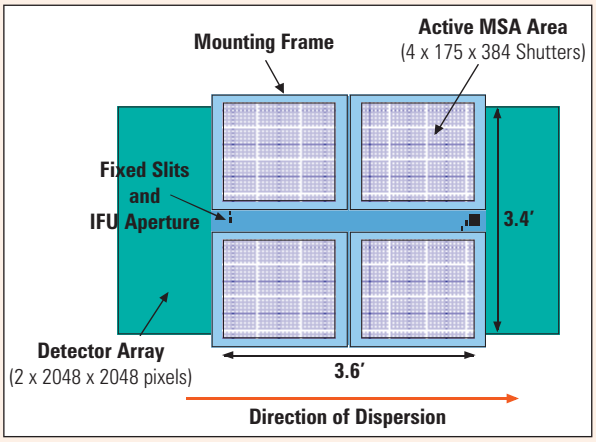


**Figure 3:** Schematic layout of the NIRSpec slit mask overlaid on the detector array projected to the same angular scale.

The NIRSpec slit-selection mechanism is a programmable Micro Shutter Array (MSA) to be provided by NASA. The MSA is made up of four 384-by-175 sub-arrays of individually programmable shutters. The open area of each shutter is 200 mas wide and 450 mas high, spaced at 250 mas in the dispersion direction and 500 mas perpendicular to the dispersion. The active area of the MSA spans a field of view covering $9^2$ arcminutes on the sky. In addition to the programmable micro shutters, the MSA also carries several fixed slits, which can be used for high contrast observations of single objects at any of the three spectral resolutions. Finally, a passive, image-slicer-based IFU, sampling a 3" x 3" field of view at 75 mas spatial resolution, is also included for use with the three $R\sim3000$ gratings. The fixed-slit and IFU modes also serve as single-object back-up modes in case of a failure of the MSA and/or partial loss of the detector array.

The NIRSpec detector system consists of two butted 2k-by-2k Rockwell HgCdTe detector arrays, which will also be provided by NASA. In order to optimize the detector-noise-limited, faint-end sensitivity of NIRSpec, the detector samples the spectra at a relatively coarse 100 mas per pixel.

NIRSpec is presently projected to be capable of reaching continuum fluxes approaching ~125 nJy at $S/N\sim10$ in $t\sim10^4$ s in $R\sim100$ mode and line fluxes as faint as $\sim5 \times 10^{-19}$ erg s$^{-1}$ cm$^{-2}$ at $S/N\sim10$ in $t\sim10^5$ s in $R\sim1000$ mode.

Scientific oversight of the NIRSpec development will be provided by the IST, whose six external European members were selected in response to an Announcement of Opportunity released by ESA in March. The NIRSpec IST, including its ESA, NASA, and Space Telescope Science Institute (STScI) ex-officio members, consists of:

Santiago Arribas (STScI/IAC)

Andrew Bunker (Exeter)

Stephane Charlot (IAP)

David Crampton (HIA)

Marijn Franx (Leiden)

Peter Jakobsen (ESA/ESTEC) - Chair

Roberto Maiolino (Arcetri)

Harvey Moseley (NASA/GSFC)

Bernie Rauscher (NASA/GSFC)

Mike Regan/Jeff Valenti (STScI)

Hans-Walter Rix (MPIA)

The NIRSpec IST replaces the previous NIRSpec Study Science Team and will remain in place through instrument commissioning in orbit and completion of the NIRSpec Guaranteed Time Observer program. Ω

# News from the Multi-mission Archive at Space Telescope

**R. Somerville,** *somerville@stsci.edu*, **for the MAST team**

As of September 1, 2004, the archive contained about 20 Tb of data. Over the past four months, MAST has distributed on average about 44 Gb of data per day. Median retrieval rates for *Hubble* and *Far Ultraviolet Spectroscopic Explorer* (*FUSE*) data have remained around 30 minutes during this period.

### User survey

MAST will be conducting its annual user survey this fall. We encourage all of our users to help us improve our services by taking a few minutes to complete the survey, which will be sent out by email. The results will be publicized after we compile the responses.

### StarView upgrade

In July, we upgraded StarView, our most flexible archive browsing and research-analysis tool, to version 7.3. StarView provides an easy-to-use, highly capable user interface, which runs on any Java-enabled platform as a stand-alone application. StarView is used to search MAST for scientific data from multiple missions, including *Hubble*, *FUSE*, *International Ultraviolet Explorer* (*IUE*), and *Extreme Ultraviolet Explorer* (*EUVE*). Users can also use StarView to examine calibrations used for a particular data set and to look for proposal information for past *Hubble* projects. Version 7.3 features protocols to aid users behind strict firewalls, improved database connectivity, and many improvements that enhance performance, reliability, and usability. Please visit **http://starview.stsci.edu/html/** to download or learn more about StarView.

### New searchable interface for HLSPs

Most MAST users are now familiar with MAST's growing collection of High Level Science Products (HLSPs), which include processed images and spectra, object catalogs, and atlases of spectra and images. We have reorganized our HLSP page and implemented a new search engine to make it easier for users to find a specific, or to discover new, HLSPs. Go to **http://archive.stsci.edu/hlsp/index.html** to explore it.

### New HLSPs

The Galaxy Evolution from Morphology and Spectral energy distributions (GEMS) project (PI Hans-Walter Rix) imaged an area of about 800 square minutes of arc on the sky with *Hubble*'s Advanced Camera for Surveys (ACS). This contiguous field, centered on the Chandra Deep Field South, contains roughly 10,000 galaxies down to a depth of 24$^{th}$ magnitude in the *R*-band. For those 10,000 objects, accurate photometric redshifts in the range $0.2<z<1.2$ are available from the COMBO-17 project. MAST will soon release HLSPs from GEMS, including the reduced mosaic of 9-by-9 ACS pointings in the F606W and F850LP filters, the object catalogs, and the redshift data. We expect the release to occur this fall. Check **http://archive.stsci.edu/hlsp/index.html** for updates.

A mean quasar spectrum from 630–1156 Å was constructed by Scott et al. (to appear in the November 2004 issue of *The Astrophysical Journal*) from 128 *FUSE* observations of 85 active galactic nuclei with redshifts $z < 0.67$. The composite quasar spectrum is now available as a HLSP at **http://archive.stsci.edu/prepds/composite_quasar/**.

The Archival Pure Parallel Program (APPP; PI: Casertano) is processing and combining about 2,000 images from the Wide Field and Planetary Camera 2, primarily in the wide *UBVI* filters, obtained in parallel with other *Hubble* instruments. The APPP team has now made available a first release (v0.5) of HLSPs, consisting of combined, drizzled, cosmic-ray cleaned images from the Large and Small Magellanic Clouds and the halos of nearby galaxies. Visit **http://www-int.stsci.edu/~yogesh/APPP/** to find out more or to download the data.

### New GOODS HLSP page and browse page

The Great Observatories Origins Deep Survey (GOODS) project has a new HLSP page, with links to the HLSP as well as other pertinent sites: **http://archive.stsci.edu/prepds/goods/**. A new tool is available for browsing the GOODS images at **http://archive.stsci.edu/prepds/goods/goods-cdfs.html**. With this browse tool, users can click on any GOODS tile and see or download a color jpg or tiff image of that region.

*Continued page 18*

MAST from page 17

**New search page for VLA FIRST co-added Images**

MAST has added a new search page for the co-added data from the VLA Faint Images of the Radio Sky at Twenty-cm (FIRST) project: **http://archive.stsci.edu/vlafirst/search.php**. There are now over 29,000 files included in this on-line archive. See the updated Getting Started page for more information about how to retrieve these data (**http://archive.stsci.edu/vlafirst/getting_started.html**)

**Virtual Observatory summer school**

In September, the US National Virtual Observatory (VO) Project held the first Applications Software Development Summer School, sponsored by the NSF and NASA, at the Aspen Center for Physics in Aspen, Colorado. The faculty included many members of the Institute- and JHU-based National Virtual Observatory (NVO) group. In this one-week course, students learned how to work with the standard software developed by the NVO and International Virtual Observatory Alliance. In addition, they learned techniques for creating VO services, both on the server and client side, and methods for interfacing programmatically to the Institute's VO Registry. The Institute sponsored a Twiki site for web-collaborative development of the course. Students used this site to access all the required software, exercises and references to other documents. For more information, see **http://www.us-vo.org/summer-school/index.cfm**. Ω

# James A. Westphal

**S. P. Maran,** *maran@aas.org*

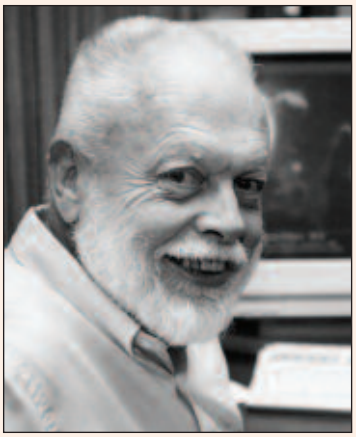

**Jim Westphal**, Principal Investigator for *Hubble*'s original Wide Field & Planetary Camera. Photo supplied by Robert Paz (Caltech).

Jim Westphal died on September 8, 2004. He is the first of the original Space Telescope science instrument Principal Investigators to leave us. The future orbiting observatory was just "*ST*" and not yet "*Hubble*" when Jim and other members of the original Science Working Group were selected in 1977. There was no Space Telescope Science Institute, so the instrument PIs and science teams interfaced directly with the contractors who built the spacecraft, optical telescope assembly, and ground systems, in addition to the NASA center project offices that managed this bewildering array of "associate contractors." A painting commissioned in that era for a Goddard retirement party shows a battle royal between two recognizable *ST* gladiators in a faux-Roman coliseum, with Westphal, his customary colorful plaid shirt showing around the folds of a toga, among the spectators. Jim was a force for calm and reason amidst such turmoil. At *Hubble* development meetings, he was generally the only scientist in the room without a graduate degree, but he was the one who was heard with the greatest attention. Jim's favorite adjective was "wondrous," and we all wanted to share his wonder at the phenomena of space and geophysics.

Westphal had worked as a physicist with a petroleum exploration team in a Mexican jungle and in a research lab devoted to the same enterprise. He came to Caltech and began a spectacular series of contributions to lunar, planetary, and geophysical exploration through his remarkable talents as an instrument designer. Among many achievements, his work on electronic imaging extended the reach of the 5-m Hale Telescope at a time when it was still the most powerful telescope ever made, and he brought the same innovative talent to our *Hubble* world.

James A. Westphal, B.S. in Physics, University of Tulsa, Emeritus Professor of Planetary Science at Caltech, MacArthur Fellow, designer of instruments and experiments for ground-based and space astronomy and for the exploration of geysers, volcanoes, glaciers, and the ocean depths, truly was "one of a kind" and will long be missed. Ω

# COSMOS: The Largest Cosmic Evolution Survey with the Hubble

**B. Mobasher,** *mobasher@stsci.edu*, **N. Scoville,** *nzs@astro.caltech.edu*

COSMOS is a Hubble Treasury project (PI: Nick Scoville) to perform a survey using the Advanced Camera for Surveys (ACS) in a single band (F814W (*i*-band)) in a contiguous 2 deg$^2$ equatorial field. A total of 640 *Hubble* orbits have been allocated to the COSMOS project over two cycles. In Cycle 12, 50 orbits were given over to supernova type Ia searches as requested by the TAC. The imaging survey uses 270 and 320 orbits in Cycles 12 and 13, respectively. The selection of an equatorial field has allowed observatories in both hemispheres to join forces for the extensive follow-up observations. The selected field at 10 hr has exceptionally low cirrus background (only 50% worse than the very best fields, like the Lockman Hole) and is devoid of bright ultraviolet, X-ray, and radio sources. Table 1 lists the expected number of galaxies in COSMOS to its magnitude limit. Figure 1 compares COSMOS with other large *Hubble* surveys in the depth-area parameter space.

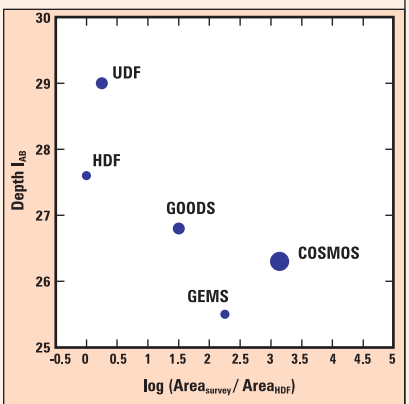


**Figure 1:** Comparison between the largest *Hubble* surveys by depth and area. Sizes of the points are proportional to the number of *Hubble* orbits awarded to each program.

The aim of COSMOS-ACS is to thoroughly map the morphology of galaxies as a function of local environment (density) and epoch, all the way from high redshift ($z > 3$) to the nearby ($z < 0.5$) Universe. Substantial large-scale structure (LSS) exists on scales up to 100 Mpc (co-moving), influencing galaxy evolution and morphological mix. Therefore, the field size is adopted to encompass co-moving areas of 50-by-50 Mpc at $z=0.5$, 137-by-137 Mpc at $z=2$, and 170-by-170 Mpc at $z=3$, fully sampling all scales currently envisaged for LSS. Figure 2 shows simulated results for a 2 deg$^2$ area at $z=1$ and $z=2$, illustrating the evolution of galaxies and clusters and formation of LSS between these redshifts. The co-moving volume (out to $z=4$) covered by the COSMOS is 9 x 10$^7$ Mpc$^3$, comparable to those sampled in the local universe by the Sloan and 2dF surveys. Imaging in F814W is sufficiently deep to fully characterize morphology, multiplicity, and interaction of L* galaxies to $z\sim2$ ($i\sim25$ mag), measure structural parameters of galaxies (asymmetry, concentration), and perform bulge-disk decomposition.

**Table 1. Number of expected galaxies in COSMOS**

| Class | Expected Number | F(814w) mag limit | Note or reference |
|---|---|---|---|
| All objects | 1.9 x 10$^6$ | < 26.5 | Metcalf et al. 2001, *MNRAS* 323, 795 |
| AGNs | 3,400 | 26.5 | Based on Lockman Hole |
| Clusters | 100 | 5x 10$^{-17}$ | X-ray flux in erg/sec |
| EROs | 25,000 | 24.5 | Daddi et al. 2000, *A&A* 361, 535 |
| QSOs[1] | 600(100) | 24(21) | Croom et al. 2001, *MNRAS* 328, 150 |
| ULIRGs[2] | 3,000 | 25.5 | Smail et al. 2002, *MNRAS* 331, 795 |
| Red high-*z* galaxies | 10,000 | 25 | Labbé et al. 2002, *AJ* 125, 1107 ($z > 2$) |
| Lyman-break galaxies | 10,000 | 25 | Shapley et al. 2001, *ApJ* 562, 95 ($z > 2$) |

[1] Quasi-stellar objects.
[2] Ultra-luminous infrared galaxies.

Combined with the follow-up observations from space- and ground-based facilities, COSMOS should become fundamental to nearly every area of observational cosmology, including : (1) the evolution of LSS, galaxies, clusters and cold dark matter on scales up to $>10^{14}\,M_{sun}$, well sampled as a function of redshift; (2) the formation, assembly and evolution of galaxies and star formation as a function of LSS environment, morphology and redshift; (3) the full reconstruction of the dark matter distributions out to $z\sim1$ using gravitational lensing shear maps; and (4) evolution of active galactic nuclei (AGNs) and the relationship between black-hole growth and galaxy evolution.

*Continued page 20*

COSMOS from page 19

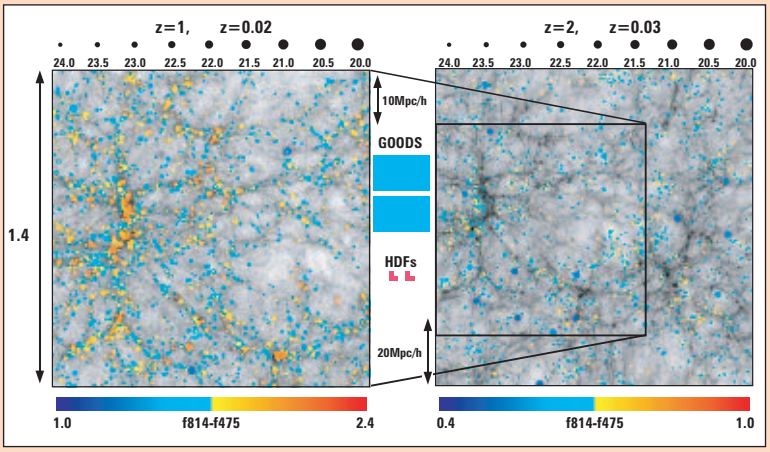


**Figure 2:** Cold dark matter (CDM) simulation results for 2 deg² at $z=1$ and $z=2$, illustrating the evolution of galaxies and clusters and the contrast between void and wall regions at both redshifts. The gray scale indicates the dark matter distribution and the symbols show luminous galaxies. The magnitudes are computed for the F814W filter. At each redshift, the depth slice is 50 Mpc, corresponding to $\Delta z = 0.02$. Also shown are the field sizes of the Hubble Deep Field (HDF) and Great Observatories Origins Deep Survey (GOODS).

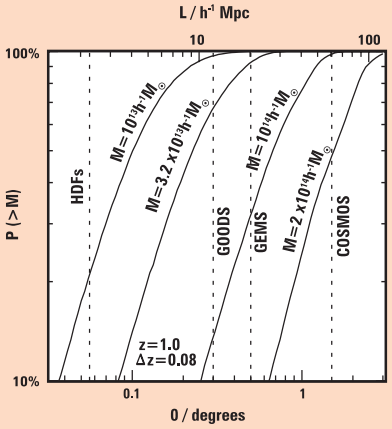


**Figure 3:** The curves, which show the probability of enclosing at least one structure of the specified mass, are shown as a function of the field size at $z=1$, from CDM simulation. From left to right, the masses correspond approximately to the Local Group, a "poor" cluster, the Virgo cluster, about 50% of the Coma cluster.

### *Hubble* observations

The *Hubble*/ACS observations are performed using one orbit/pointing (F814W=27.2 mag, 10σ) and allowing for 5% overlap between adjacent exposures. All the exposures are taken at ± 10 deg orientation. At the time of this writing, we have full coverage of approximately one deg² of the COSMOS field with the ACS. During the ACS exposures, both the Near Infrared Camera and Multi-Object Spectrometer (NICMOS) and the Wide Field and Planetary Camera 2 (WFPC2) are used as parallel instruments, obtaining exposures sampling approximately 5% and 40% of the field at 1.6 micron and ultraviolet wavelengths, respectively.

### Multi-wavelength COSMOS

Although COSMOS was initiated with the *Hubble* ACS observations, it is now a survey with extensive multi-wavelength datasets from other facilities. Table 2 shows the current status of the multi-wavelength datasets. These reduced data and catalogs will become public one year after their acquisition and will be archived at the InfraRed Science Archive at the Infrared Processing and Analysis Center. We are completing full coverage of the COSMOS in X-ray (*X-Ray Multi-Mirror Mission*, *XMM*), ultraviolet (*Galaxy Evolution Explorer*, *GALEX*), *U*-band (Canada France Hawaii Telescope, CFHT), *BVRiz* (Subaru), *K*-band (Cerro Tololo Inter-American Observatory, CTIO/Kitt Peak) and radio (Very Large Array). We plan additional surveys of the COSMOS field in the mid-infrared (*Spitzer*), X-ray (*Chandra*), and an extensive intermediate and narrow-band optical survey.

In September, our team completed a trial photometric redshift catalog with over 1 million objects based on the extensive ground-based imaging at Subaru (*B*, *V*, *r*, *i* & *z*), the CFHT (*U*), and the National Optical Astronomy Observatory (*Ks*). This catalog is now enabling the identification of the most massive clusters and photometric selection of objects for morphological studies.

### Science with COSMOS

The *Hubble* data, combined with supporting multi-waveband observations of the COSMOS field, will be used to address fundamental questions in observational cosmology, as follows:

*Large scale structure*. The need to sample very large scales arises from the fact that demonstrated structure exists up to a total mass of $10^{14}$ $M_{sun}$, with existing smaller surveys having a lower probability of enclosing the very large masses at $z\sim1$ (Fig. 3). The existing and on-going

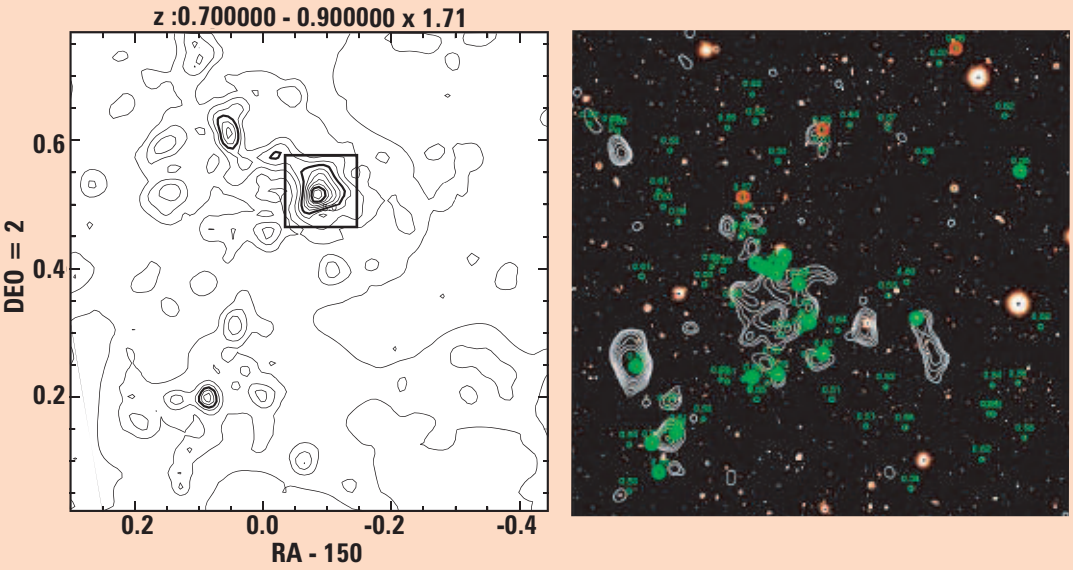


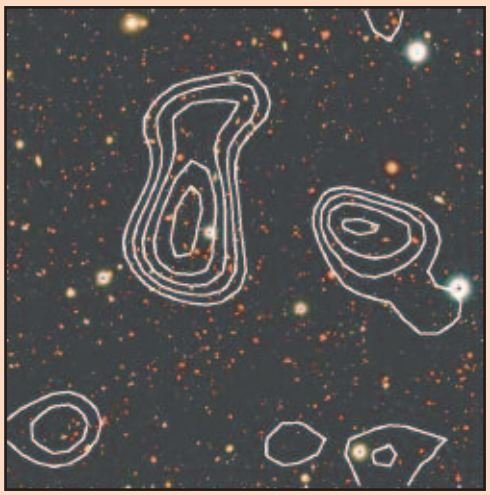

**Figure 4:** At left, large scale structures at $0.7<z<0.9$ in the COSMOS 0.7 x 0.7 deg field of view (FOV) obtained with our photometric redshift catalog, from Supreme-Cam on the Subaru telescope. In middle, cluster of galaxies at $z\sim0.7$ found from our photo-$z$ catalog around one of the *XMM* sources. X-ray contours are overlaid on Supreme-Cam $i$ band image. This cluster is spectroscopically confirmed as a real cluster by the Focal Reducer/low dispersion Spectrograph (FORS1) on the Very Large Telescope (VLT). Large green circles are galaxies around $z=0.73$. FOV is 6.7 x 6.7 arcmin. This field is shown in left panel by inset box. On right, the results of weak-lensing analysis on the same field as middle.

projects such as the Great Observatories Origins Deep Survey (GOODS) and Galaxy Evolution from Morphology and Spectral energy distributions survey (GEMS) adequately sample masses up to 3 x $10^{13}$ $M_{sun}$, whereas COSMOS is expected to sample the largest known structures $\sim$2 x $10^{14}$ $M_{sun}$ out to $z\sim1$, corresponding to Coma-size clusters.

*Assembly and evolution of galaxies*. Galaxies in the early universe are built up by two major processes: dissipational collapse and merging of lower mass protogalactic and galactic components. Their intrinsic evolution is then driven by the conversion of primordial and interstellar gas into stars, with galactic merging and interactions triggering star formation and starbursts.

The wide-area COSMOS-ACS survey will yield $10^6$ galaxies with multi-waveband color information. Combined with photometric and spectroscopic redshifts, COSMOS allows measurement of both the luminosity and 2D-3D correlation functions of galaxies of different types and their evolution with redshift and environment. This is of fundamental importance in constraining galaxy-formation scenarios. Moreover, combined with multi-waveband ground-based data, we investigate the star-formation rates and AGN activity as a function of morphology, size, redshift, and LSS environment.

*Gravitational lensing and dark matter*. Although ground-based lensing surveys are broad in areal coverage, many faint galaxy images are either unresolved or smeared by atmospheric seeing, with only the most massive lenses $>10^{14}$ $M_{sun}$ detected. The stable ACS point-spread function permits extraction of the shapes of $\sim$60 galaxies per arcmin$^2$, 3–5 times that of the best ground-based data, as demonstrated by GOODS. By conducting COSMOS in a field with available *XMM* images and redshift information to reveal galaxy groups and clusters, it will be possible to probe correlations between mass and light. Figure 4 illustrates a cluster found in COSMOS at $0.7 < z < 0.9$, identified using photometric redshifts and subsequently confirmed by the X-ray data. Preliminary results from weak-lensing analysis are also shown.

*Continued page 22*

COSMOS from page 21

COSMOS-ACS images also detect halos similar to those of clusters and groups in the *XMM* surveys. The lens-based mass estimates can then be compared with dynamical estimates from the velocity dispersion of galaxies in the halos.

*Properties of different types of galaxies*. Given the size of the COSMOS and its extensive multi-waveband data, a large number of galaxies of different types are identified and studied (Table 2).

Due to the small space density of AGNs, large-area multi-waveband surveys like COSMOS are needed to discover them in large numbers. The AGNs are identified from their associated X-ray and radio emission, optical spectra, and point-like nucleus in the ACS. COSMOS allows direct comparison of AGN and galaxy properties. The 'extremely red objects' (EROs) are identified using *V-K* colors. The wide-area coverage of the COSMOS allows study of the luminosity and correlation function of EROs at different redshift intervals. The ACS data allow study of morphology of the EROs as a function of LSS. Using the Subaru images of the COSMOS, a large number of Lyman-break galaxies are identified at $z=2$, 3, and 4. Using the ACS morphologies, the rest-frame properties of these objects, including the relation between morphology and density at different redshifts, will be investigated. Combined ultraviolet (*GALEX*) and ACS observations will allow the identification of starbursts.

**Near Future COSMOS**

The first major public release of COSMOS data and data products will occur at the January 2005 meeting of the American Astronomical Society. There will also be a special session scheduled to highlight the ongoing COSMOS research. It is our expectation that COSMOS will be a prime resource for investigations of cosmic evolution, and we look forward to the community's participation in this research and the use of these unique and spectacular data. Ω

## Table 2. List of the ancillary observations for COSMOS

| Telescope/ Instrument | Filter/ Wavelength/ energy range | Sensitivity/ Mag/ (area) | Complete/ Underway | Cycles: Orbits/ PI: time |
|---|---|---|---|---|
| *Hubble*/ACS | *814I* | 27 | C | C12–13: 581 orbits |
| *Hubble*/ACS | *475g* | 27 | C | C12: 9 orbits |
| *Hubble*/ACS | *475g* | 27 | U | C13–14: 590 orbits |
| *Hubble*/NIC3 | *160W* | 22.9 (5% area) | C | C12–13: 590 orbits |
| *Hubble*/NIC3 | *110W* | 23.2 (5% area) | U | C13–14: 590 orbits |
| *Hubble*/WFPC2 | *300W* | 26.4 | C | C12–13: 590 orbits |
| Subaru | (*B*, *r'*,*z'*) | (27, 27, 25) | C | Taniguchi: 10 nights |
| Subaru | *NB816* | 25 | C | Taniguchi: 5 nights |
| Subaru | *NB816* | 25 | U | Taniguchi: 5 nights |
| CFHT[1] | *u* | 27 | C | Sanders: 24 hours |
| CFHT | *u,I* | 26 | C | LeFevre: 12 hours |
| CFHT | *u-z* | | C | Deep Legacy Survey |
| Kitt Peak 4m | $K_s$ | 21 | C | Mobasher: 10 nights |
| CFHT | *K* | 23 (9'x9') | C | Sanders: 3 nights |
| UH-88[2] | *J* | 21 | C | Sanders: 10 nights |
| *GALEX* | FUV, NUV | 26.1,25.8 | C | Schminovich: $2x10^5$ sec |
| *XMM* | 0.5–10 keV | $10^{-15}$ cgs | C | Hasinger: $1.4x10^6$ sec |
| VLA-A[3] | 20 cm | 24 μJy | C | Schinnerer: 10 hours |
| VLA-A/C[4] | 20 cm | 8 μJy | U | Schinnerer: 260 hours |

[1] Canada-France-Hawaii Telescope
[2] University of Hawaii 88-inch telescope
[3] Very Large Array, configuration A
[4] Very Large Array, configurations A & C

# Hubble Peers Inside a Celestial Geode

In this unusual image, NASA's *Hubble Space Telescope* captures a rare view of the celestial equivalent of a geode — a gas cavity carved by the stellar wind and intense ultraviolet radiation from a hot young star. Real geodes are baseball-sized, hollow rocks that start out as bubbles in volcanic or sedimentary rock. Only when these inconspicuous round rocks are split in half by a geologist do we get a chance to appreciate the inside of the rock cavity that is lined with crystals. In the case of *Hubble*'s 35 light-year diameter "celestial geode" the transparency of its bubble-like cavity of interstellar gas and dust reveals the treasures of its interior.

**http://hubblesite.org/newscenter/newsdesk/archive/releases/2004/26/**

***Image Credit:*** NASA, ESA, Y. Nazé (University of Liège, Belgium) and Y.-H. Chu (University of Illinois, Urbana)

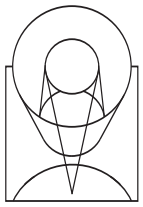

# Contact STScI:

The Institute's website is: `http://www.stsci.edu`

Assistance is available at *help@stsci.edu* or 800-544-8125. International callers can use 1-410-338-1082.

For current *Hubble* users, program information is available at:

`http://presto.stsci.edu/public/propinfo.html`.

The current members of the Space Telescope Users Committee (STUC) are:

| | |
|---|---|
| David Axon, RIT | Karen Meech, IfA |
| Martin Barstow, U. of Leicester | Peter Nugent, LBL |
| Martin Elvis, Harvard-Smithsonian | C. Robert O'Dell, U. Vanderbilt |
| Debbie Elmegreen (chair), Vassar C. | Regina Schulte-Ladbeck, U. Pittsburgh |
| Eric Emsellem, CRAL | Lisa Storrie-Lombardi, Caltech |
| Laura Ferrarese, Rutgers U. | Monica Tosi, OAB |
| Pat McCarthy, OCIW | Donald G. York, U. Chicago |

The Space Telescope Science Institute Newsletter is edited by Robert Brown, *rbrown@stsci.edu,* who invites comments and suggestions.

Technical Lead: Christian Lallo, *clallo@stsci.edu*
Contents Manager: Sharon Toolan, *toolan@stsci.edu*
Design: Krista Wildt, *wildt@stsci.edu*

To record a change of address or to request receipt of the Newsletter, please send a message to *address-change@stsci.edu.*


# ST-ECF Newsletter

The Space Telescope—European Coordinating Facility publishes a newsletter which, although aimed principally at European Space Telescope users, contains articles of general interest to the *HST* community. If you wish to be included in the mailing list, please contact the editor and state your affiliation and specific involvement in the Space Telescope Project.

**Richard Hook *(Editor)***

Space Telescope—European Coordinating Facility
Karl Schwarzschild Str. 2
D-85748 Garching bei München
Germany
E-Mail: *rhook@eso.org*

# Contents:



# Calendar

***Cycle 13***

Space Telescope Users Committee meeting . . . . . .18–19 November, 2004
Space Telescope Institute Council meeting . . . . . .23–24 November, 2004
New Cycle 13 (STIS replacement) GO budgets due . . . . . .30 November, 2004
APT for Cycle 14, Phase I released . . . . . .1 December, 2004
Cycle 14, Phase I proposals due . . . . . .21 January, 2005
Space Telescope Institute Council meeting . . . . . .7–8 February, 2005

***Mini-Workshop***

Missing Baryons . . . . . .7–9 March, 2005

***Spring Symposium***

A Decade of Extrasolar Planets Around Normal Stars . . . . . .2–5 May, 2005

SPACE TELESCOPE SCIENCE INSTITUTE


NON PROFIT
U.S. POSTAGE
PAID
PERMIT NO. 8928
BALTIMORE, MD



3700 San Martin Drive, Baltimore, Maryland 21218



STScI N-04-04